Precision Measurement of the Monthly Cosmic Ray Fluxes with the Alpha Magnetic Spectrometer

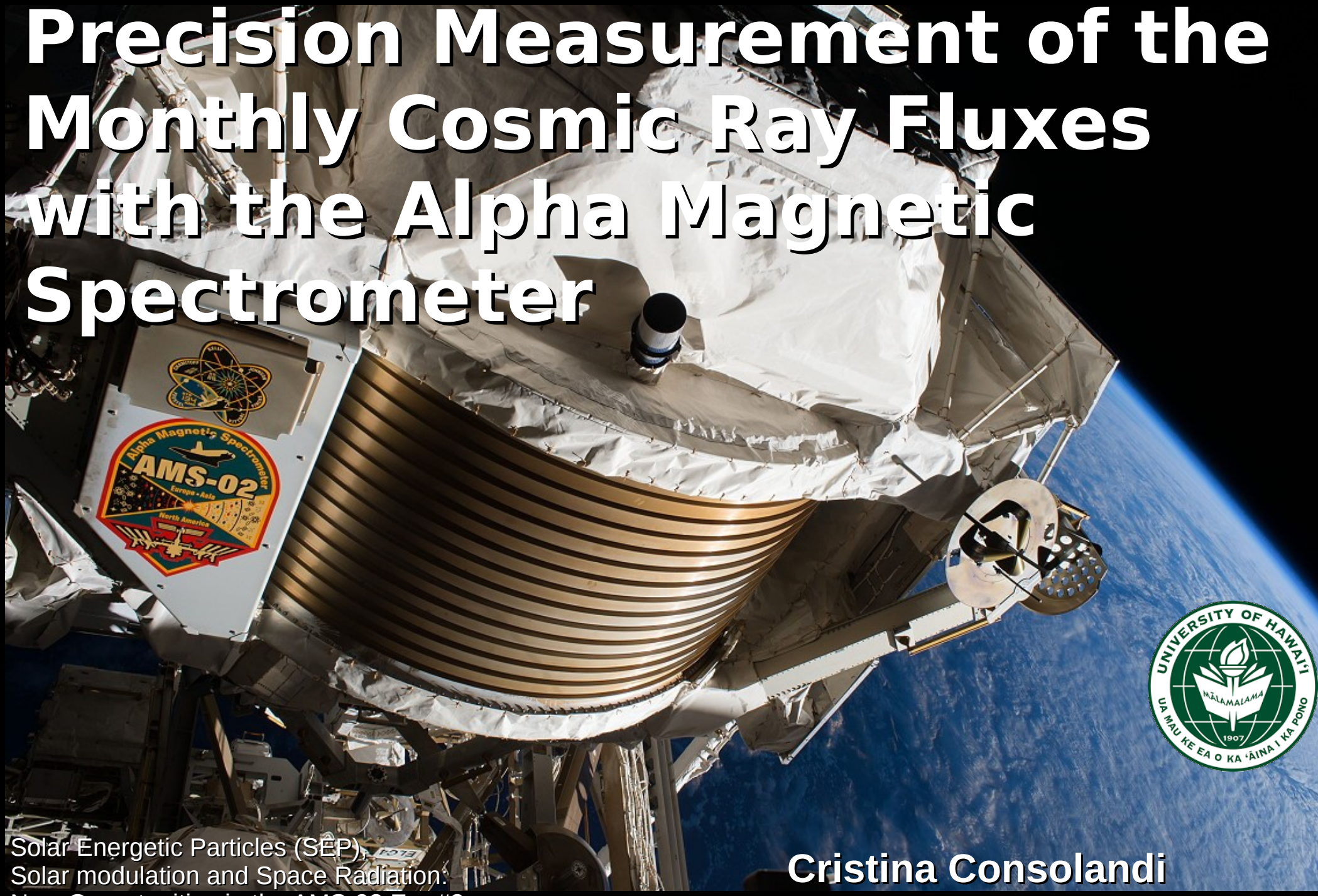

Solar Energetic Particles (SEP), Solar modulation and Space Radiation: New Opportunities in the AMS-02 Era #3
Washington DC, April 23-26, 2018

Cristina Consolandi
On behalf of the AMS Collaboration

AMS Period of Observation

AMS is a TeV precision, multipurpose, magnetic spectrometer, on the ISS since May 2011.

AMS is measuring GCR fluxes and their time variation. AMS will study the solar modulation effect and the short-term solar activity in the present (24th) and next solar cycle for the live-time of the ISS.

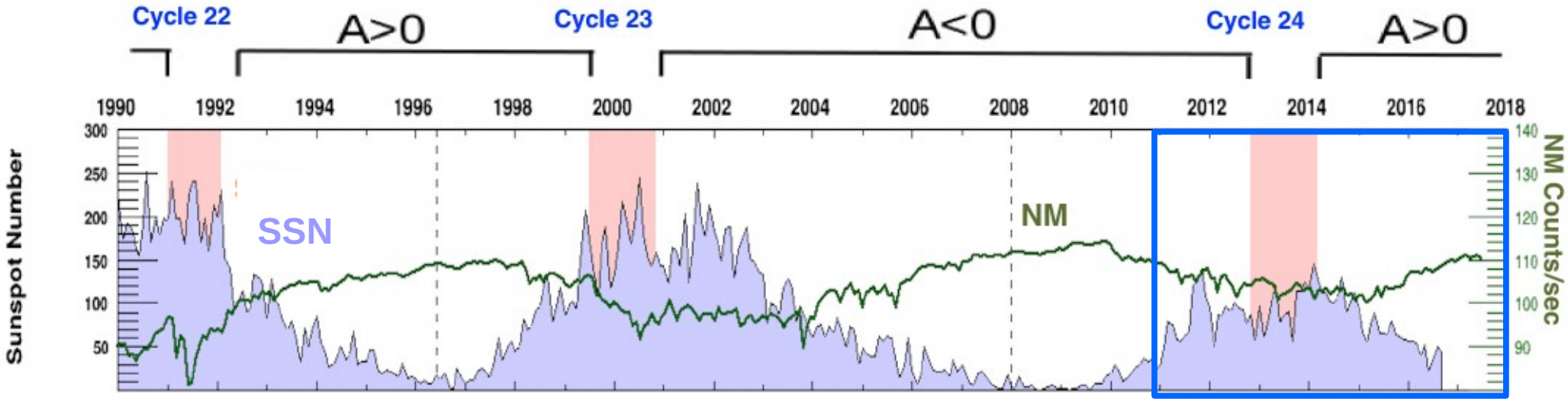

AMS: Since May 2011

Daily sunspot number: http://www.sidc.be/silso/datafiles
NMDB database at http://www.nmdb.eu

AMS Contribution to Solar Modulation

- Simultaneous multi-particle measurements.
- Fine rigidity resolution.
- Total uncertainty at the percentage level.
- Short integration time.
- Continuous particle measurement over one solar cycle.

Detailed time evolution of GCR during both periods of maximum and minimum of solar activity.

AMS measurements will help to understand the propagation of charged particles in heliosphere and to test diffusion and drift models.

AMS Detector and Proton and Nuclei Identification

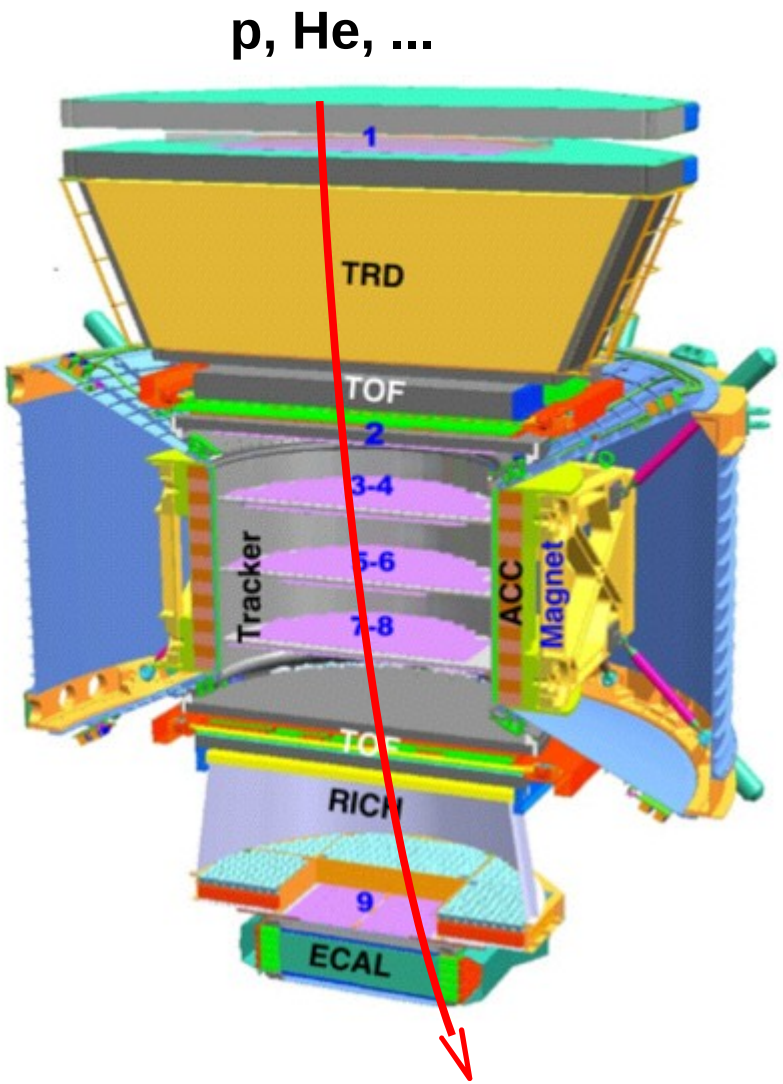

Transition Radiation Detector
- e+ e- identification

Time-of-Flight counter
- Trigger
- Velocity
- Particle flight direction
- Charge

Silicon Tracker + Magnet
- Rigidity
- Charge & sign

Ring Imaging Cherenkov detector
- Velocity
- Charge

Electromagnetic Calorimeter
- e+ e- identification
- e+ e- Energy

AMS Proton, Helium & other Nuclei

In 7 year of operation, AMS has collected more than **117 billion events**

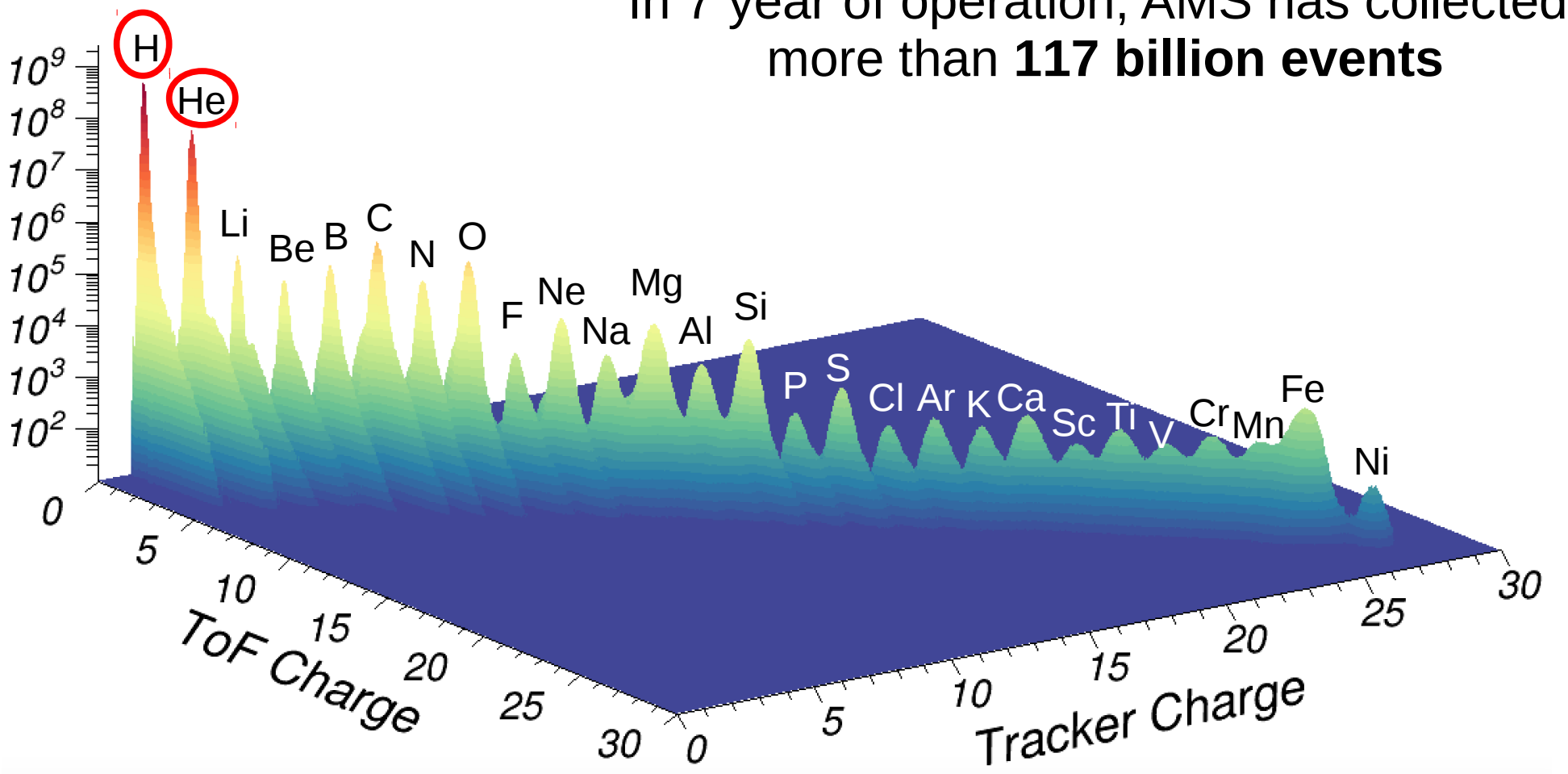

AMS Proton and Helium Fluxes vs. Time & Rigidity

Proton

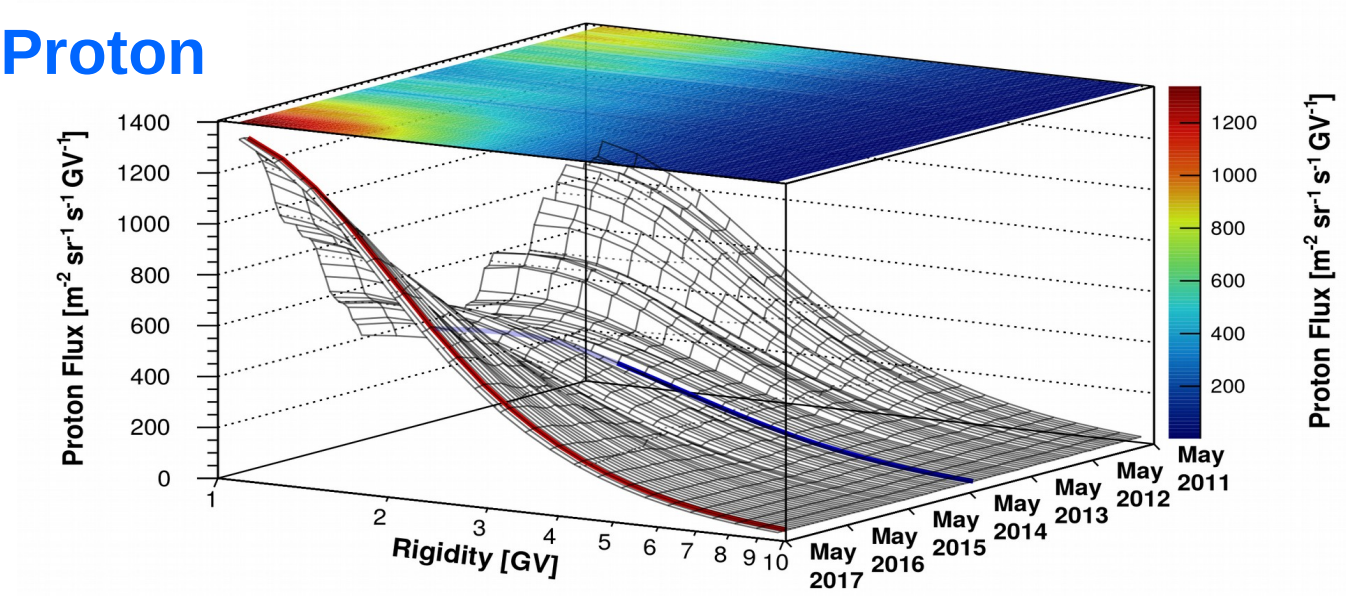

May 2011- May 2017

Helium

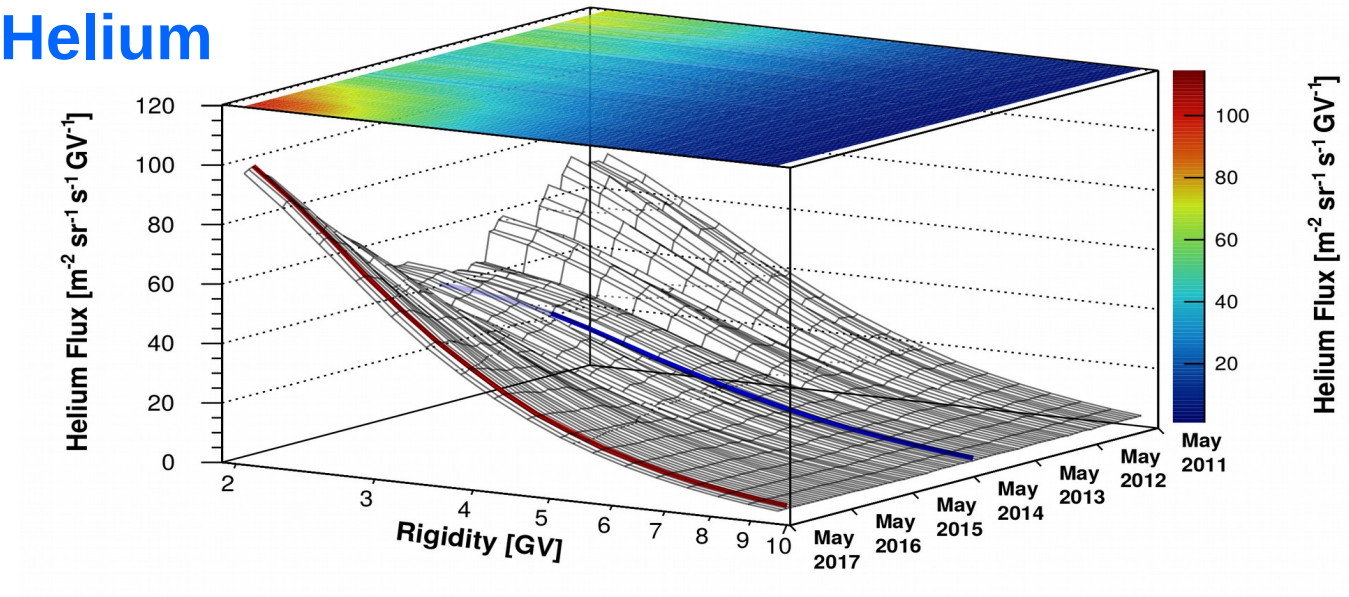

AMS Monthly Proton and Helium Fluxes (27 days, Bartels Rotation) Relative Variation

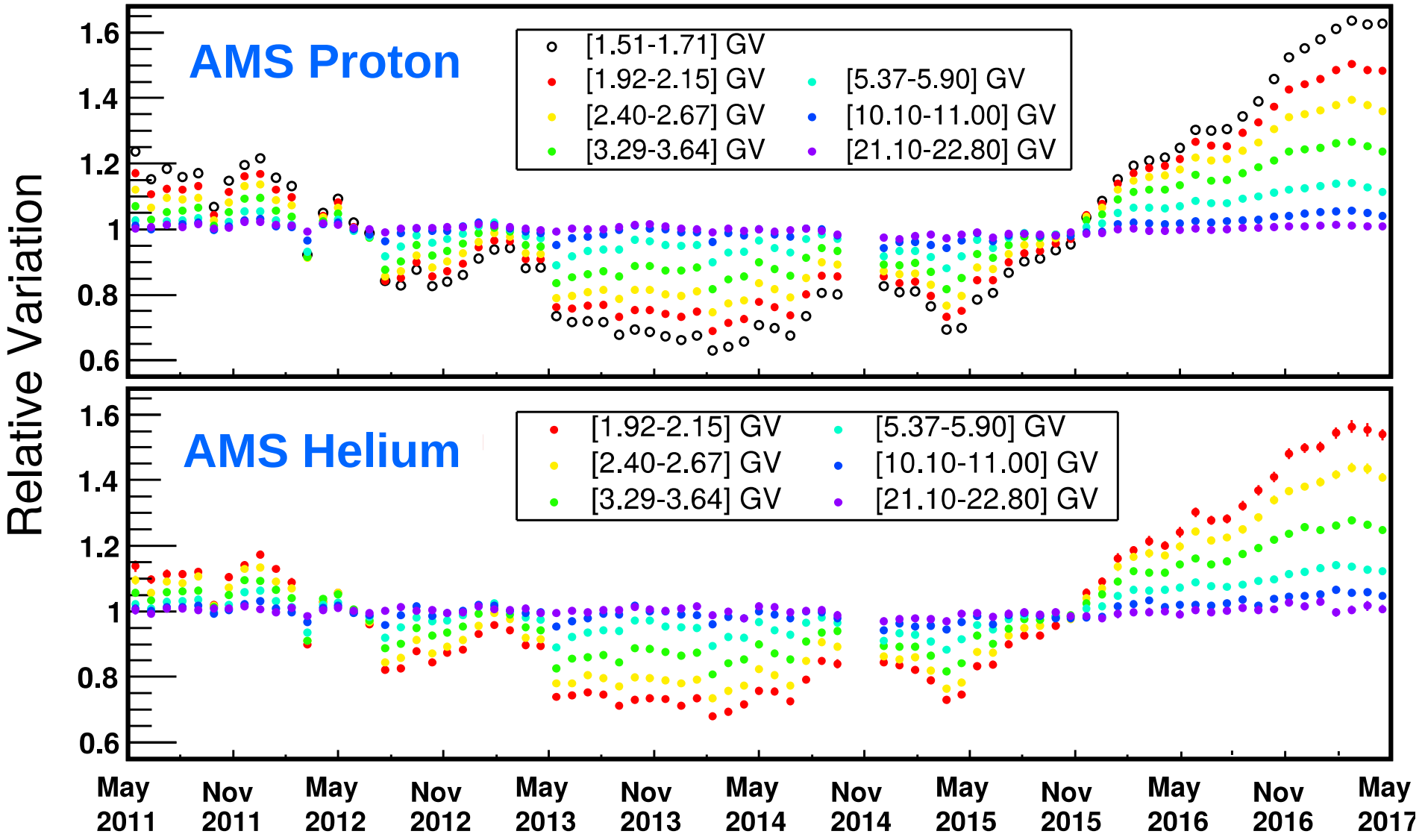

AMS Monthly Proton and Helium Fluxes Time Profiles

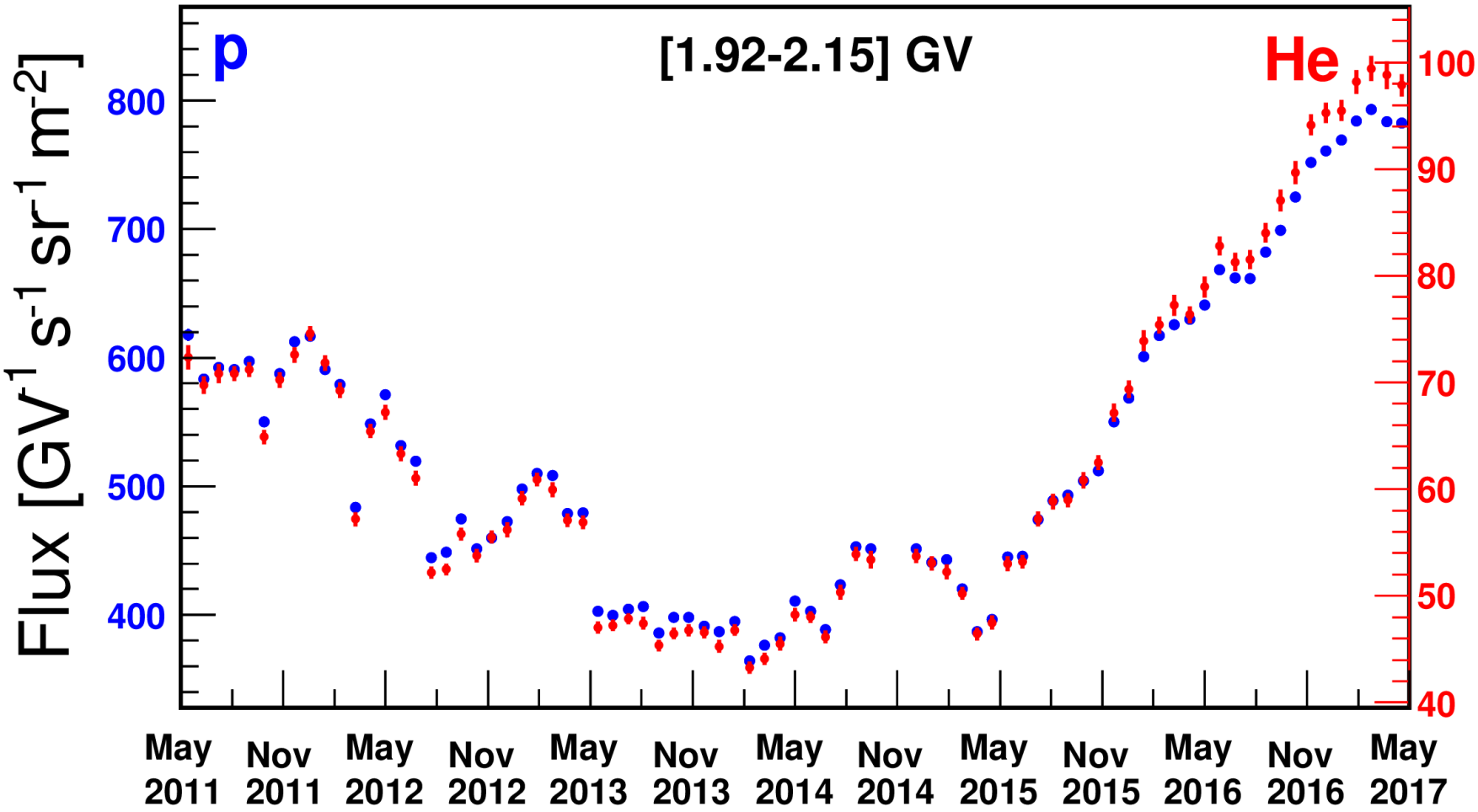

AMS Monthly Proton and Helium Fluxes Time Profiles

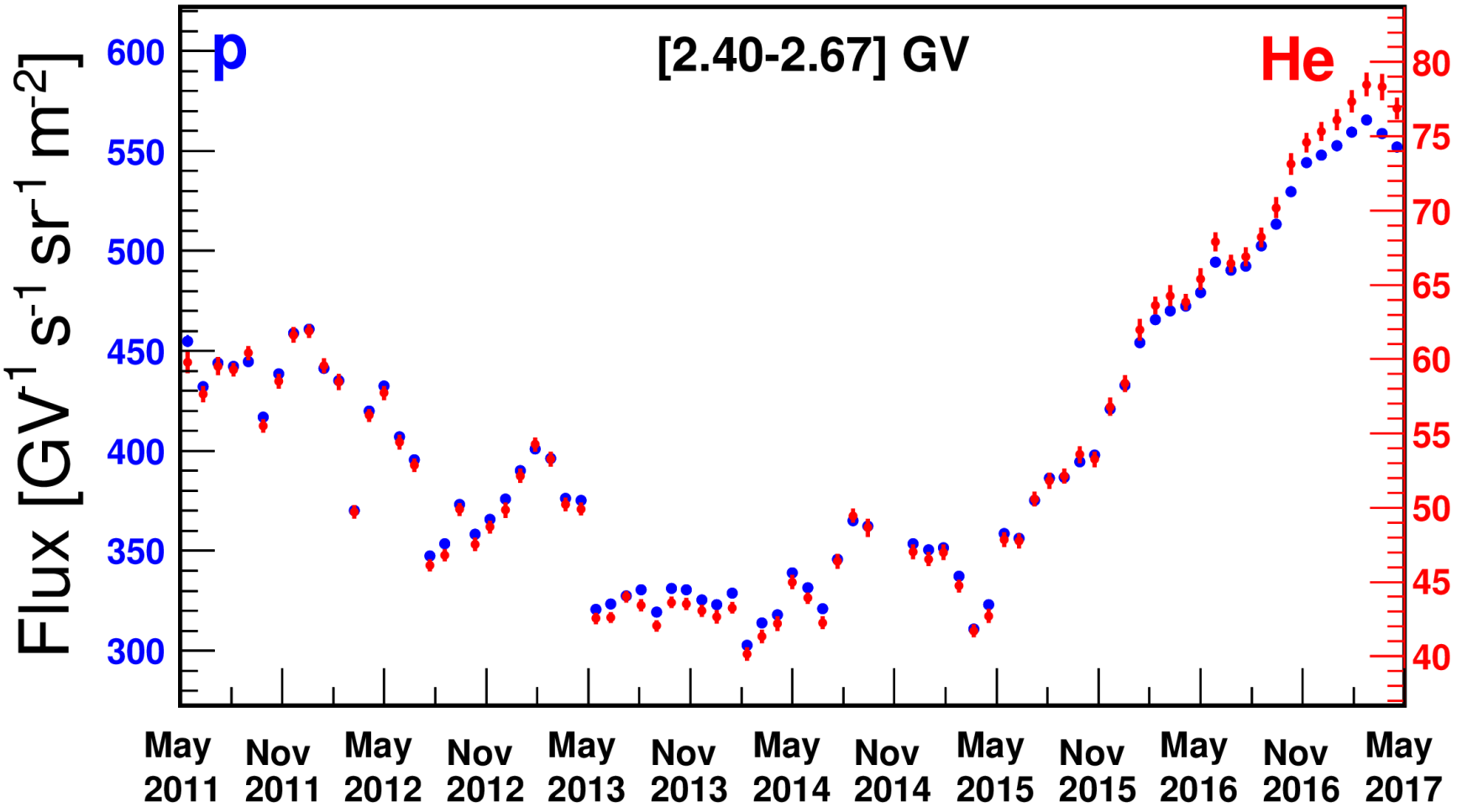

AMS Monthly Proton and Helium Fluxes Time Profiles

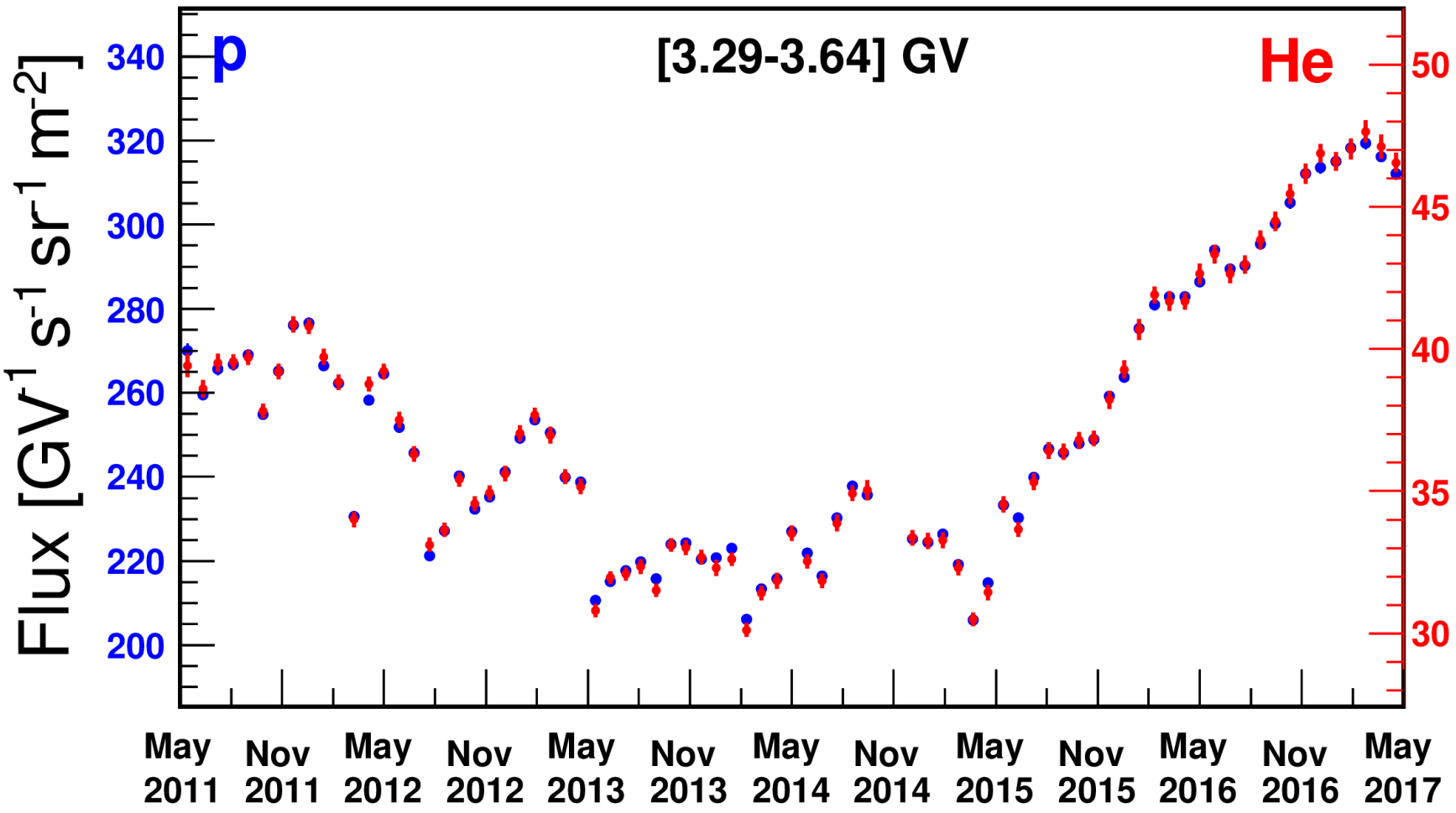

AMS Monthly Proton and Helium Fluxes Time Profiles

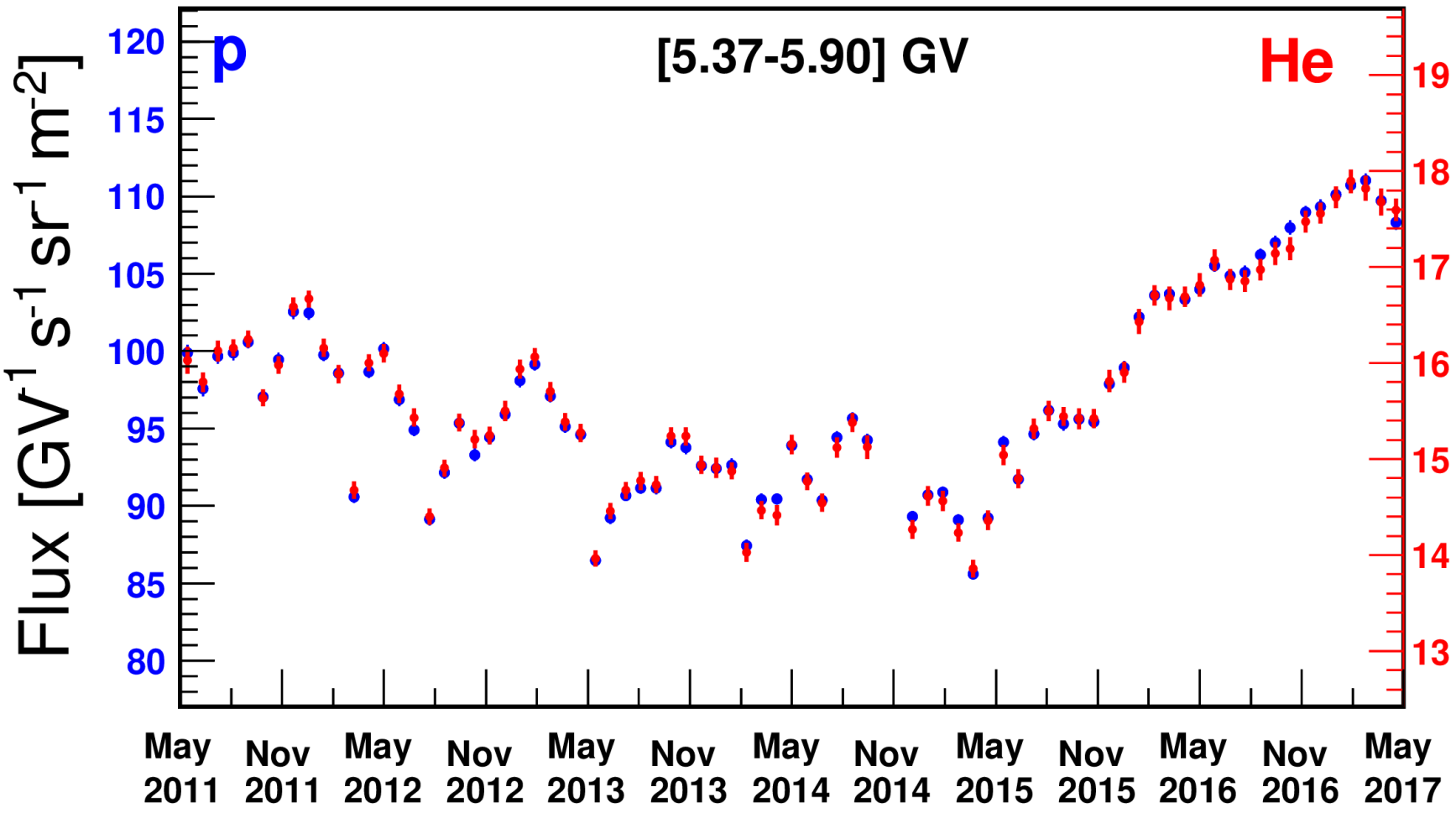

AMS Monthly Proton and Helium Fluxes Time Profiles

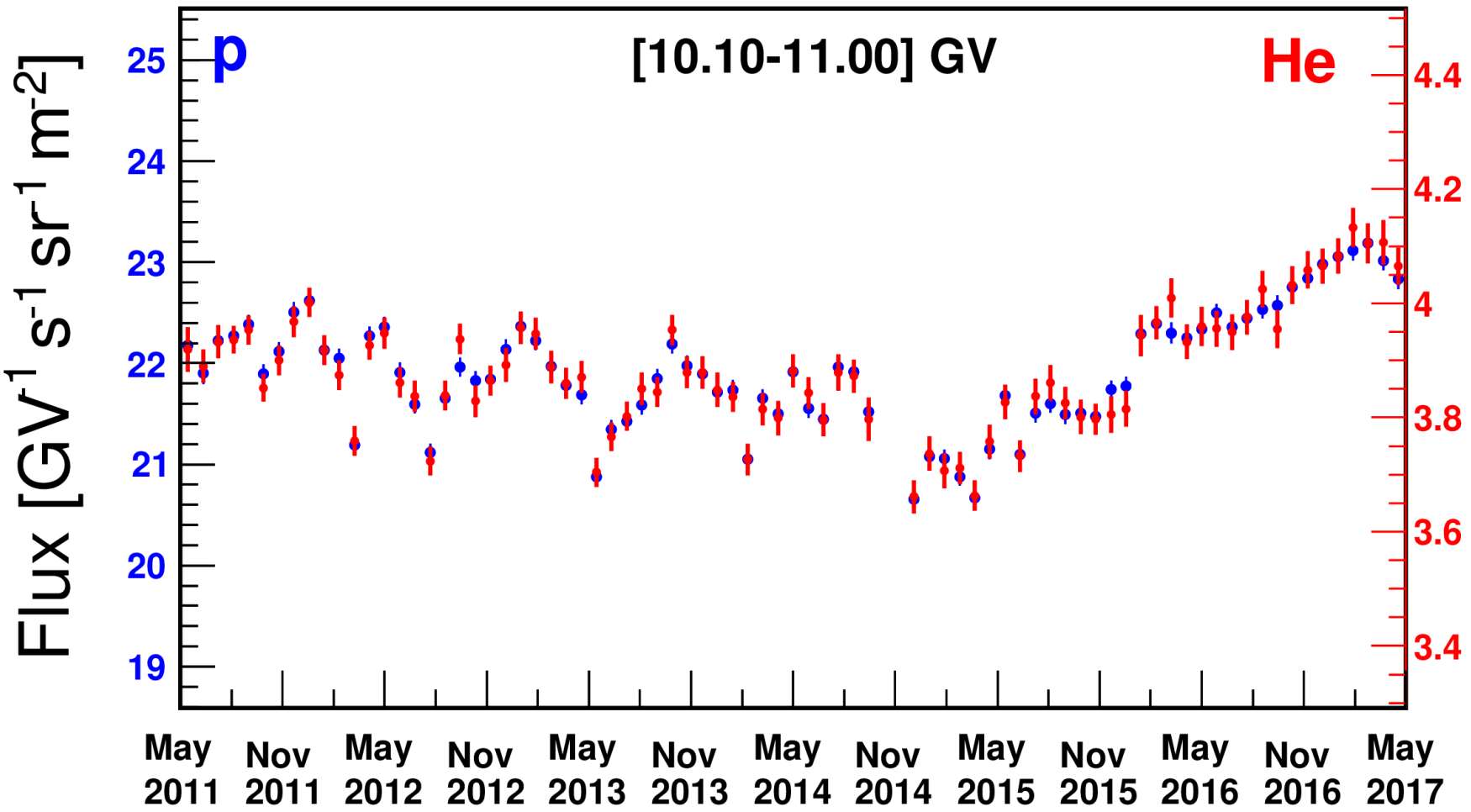

AMS Monthly Proton and Helium Fluxes Time Profiles

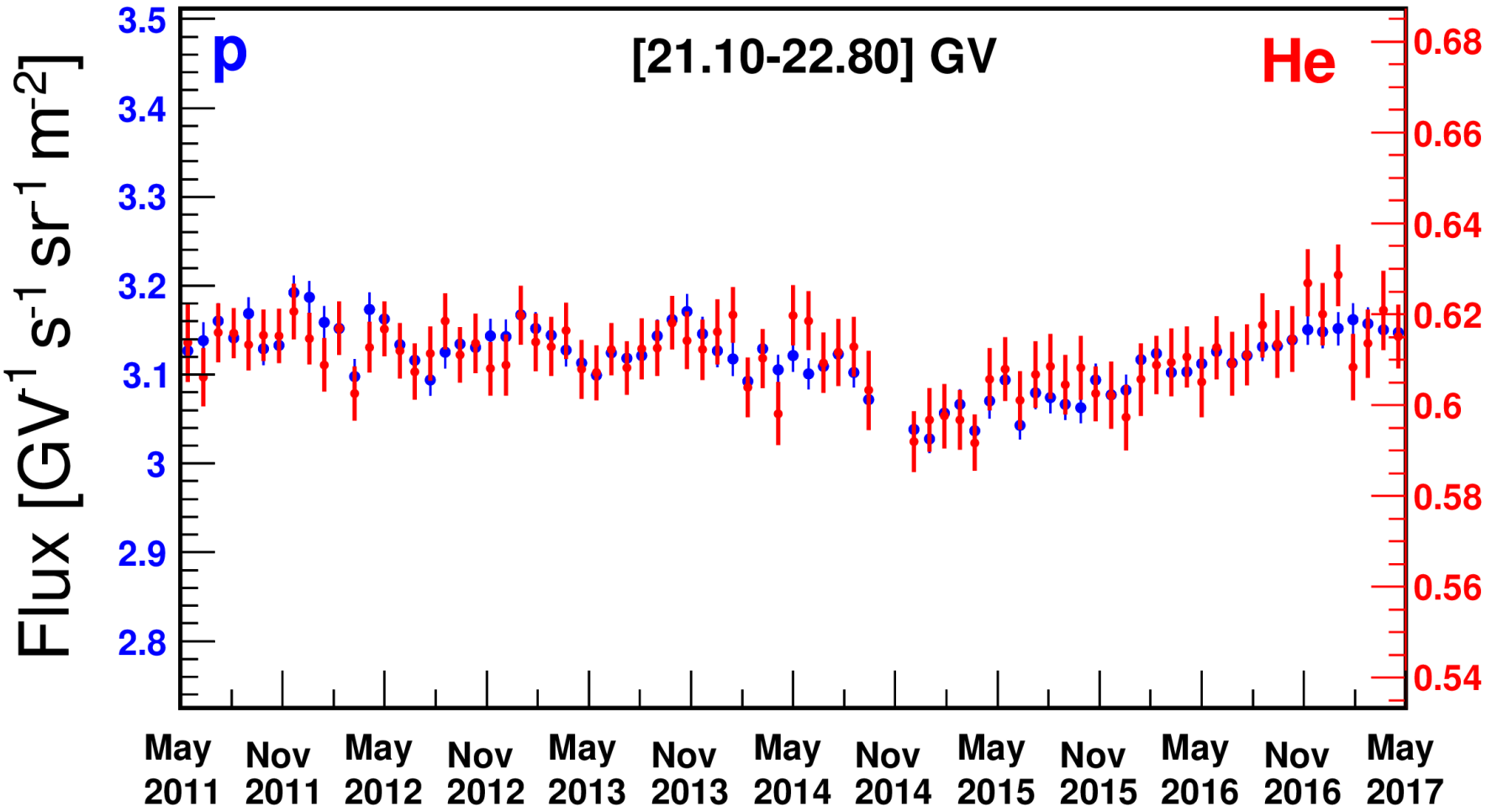

AMS Monthly Proton and Helium Fluxes Time Profiles

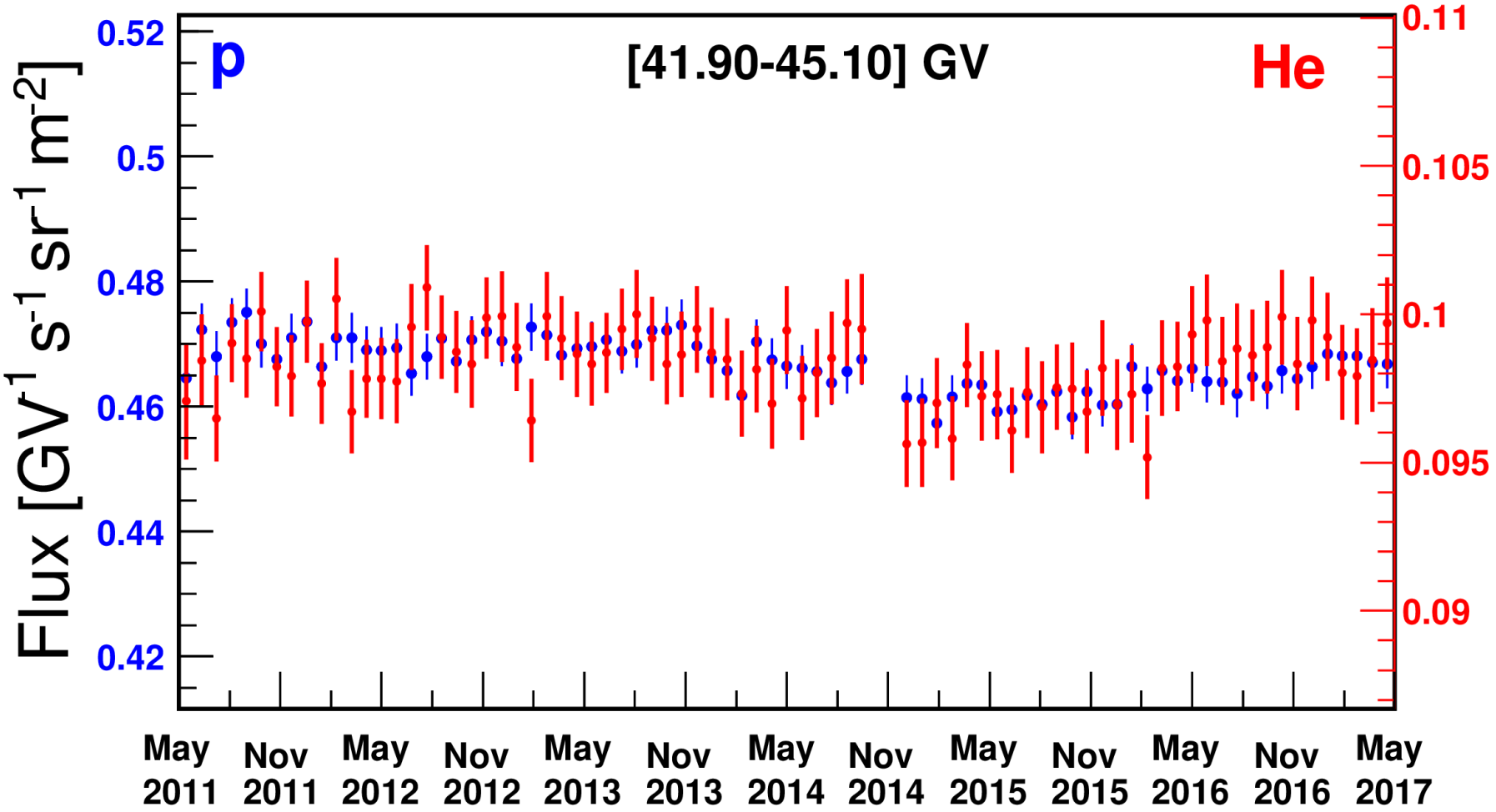

AMS Monthly Proton and Helium Fluxes Time Profiles

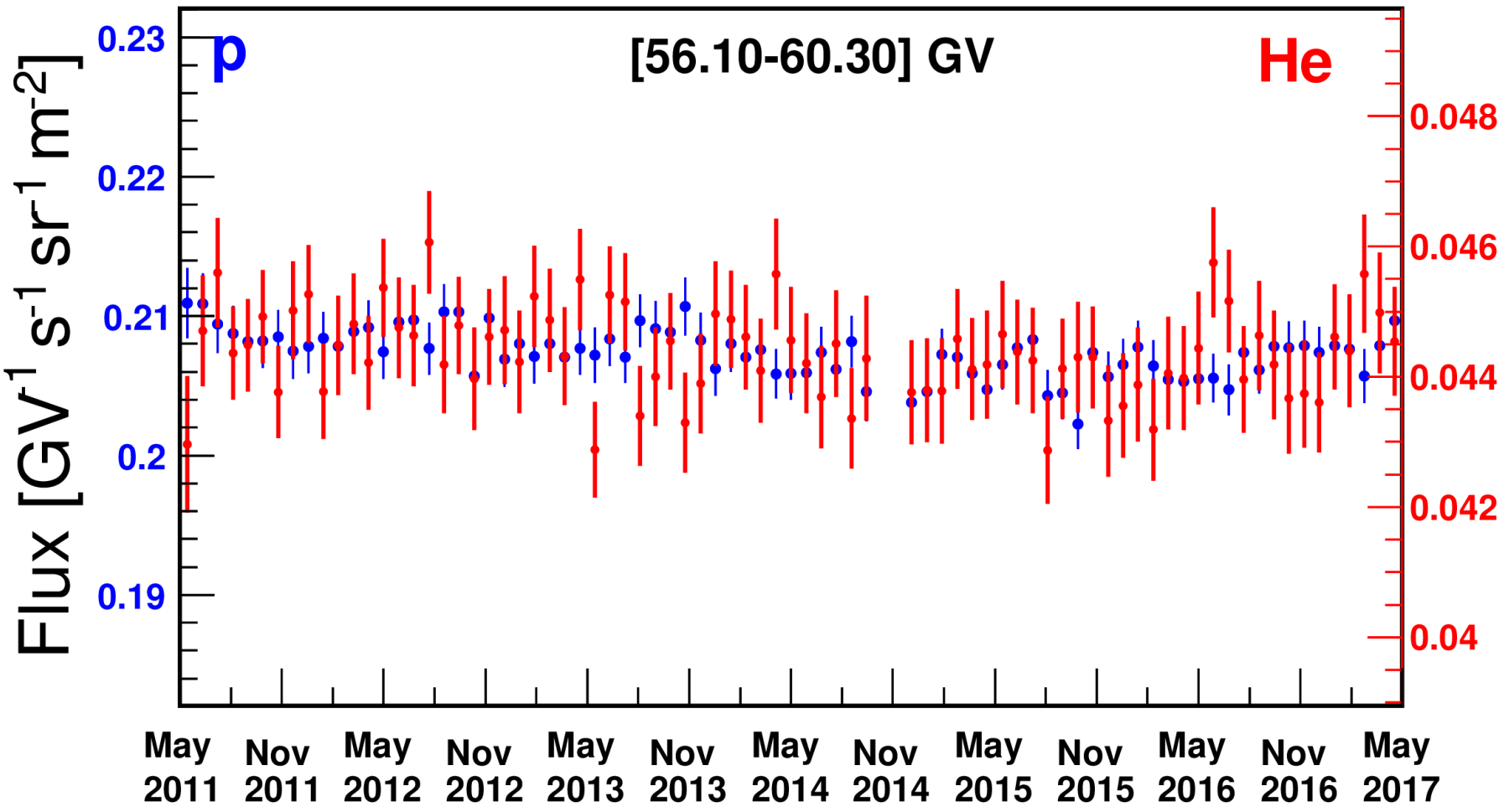

AMS Proton and Helium Low Energy Structures

- Detailed structures (green area) are clearly present below 40 GV.
- The amplitude of the structures decreases with increasing rigidity.
- Vertical dashed lines delimit boundaries of p and He structures (from I to X).
- The red vertical dashed lines denote structures that have also been observed by AMS in the electron and positron fluxes.

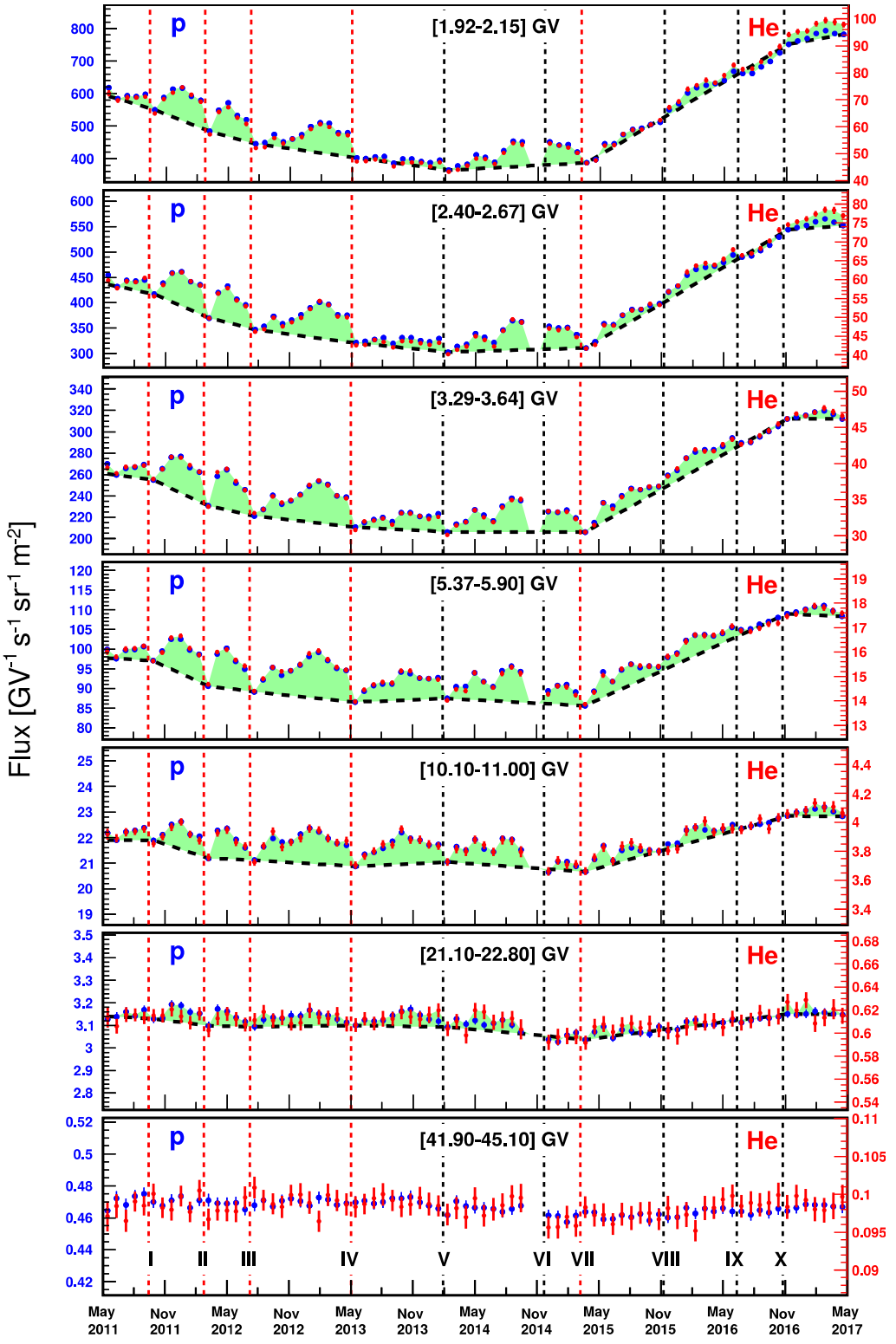

AMS Monthly p/He Flux-Ratio

Above 3 GV the p/He flux ratio is time independent

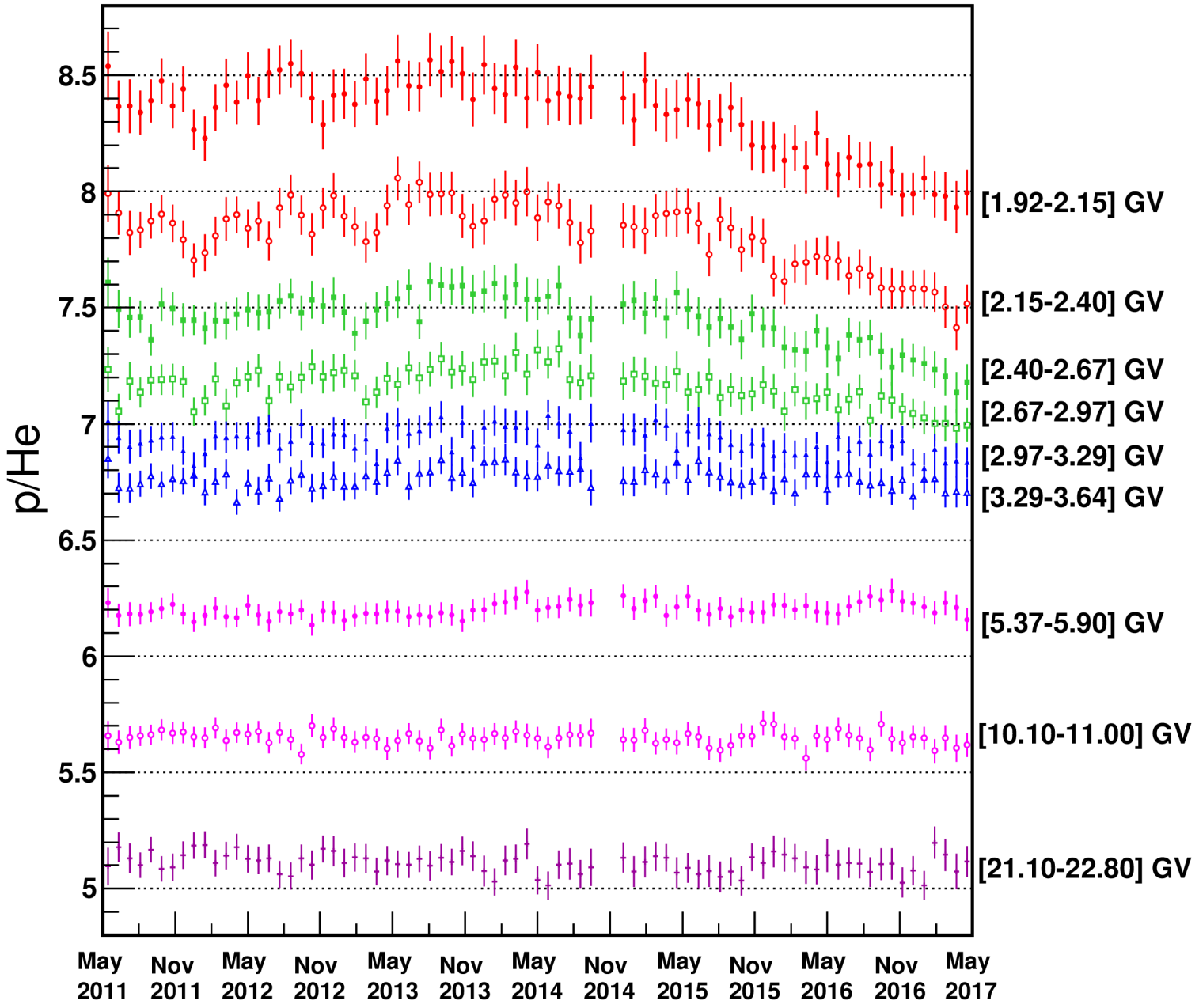

AMS Monthly p/He Flux Ratio

Below 3 GV the p/He flux ratio has a long-term decrease

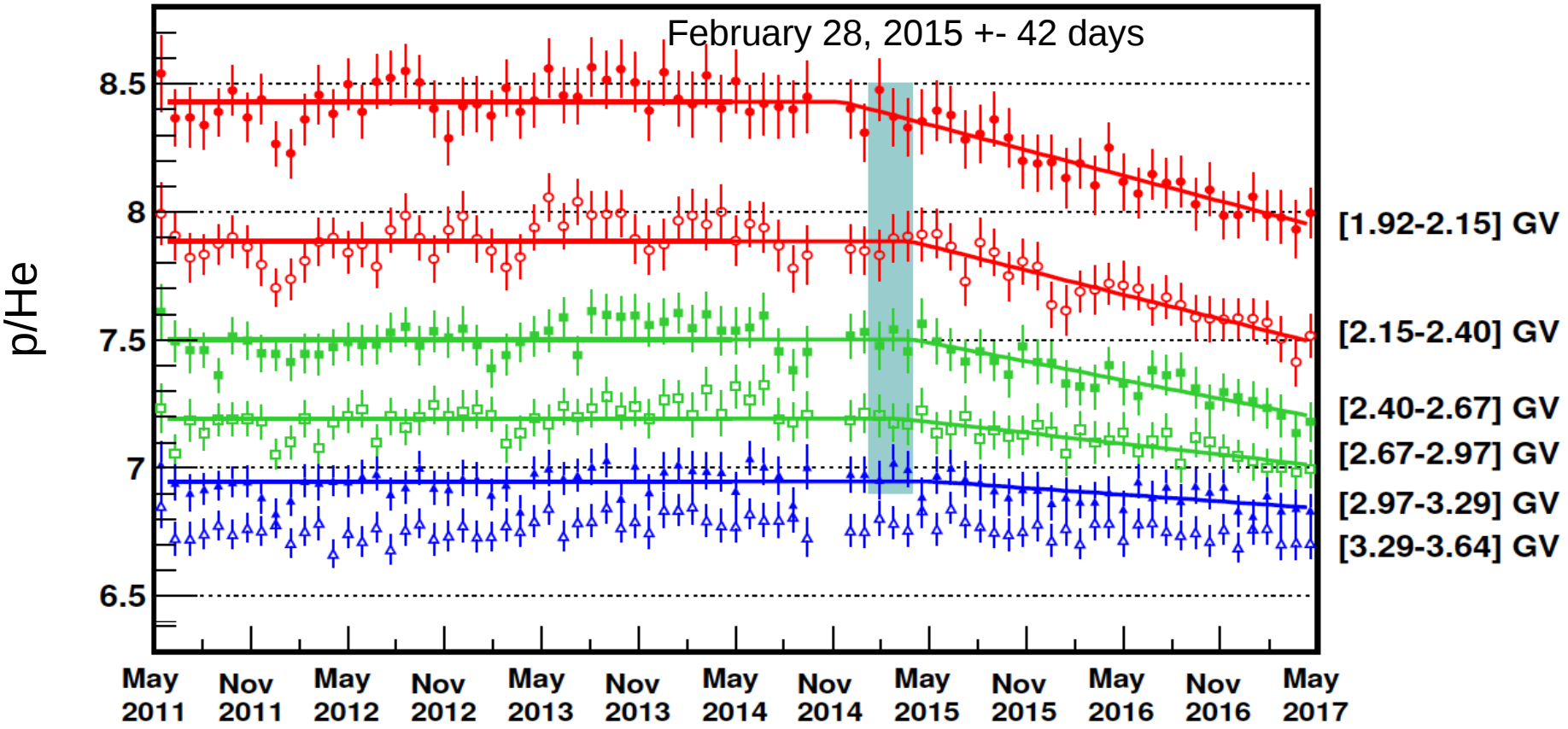

- Differences in p and He diffusion coefficients.
- Differences in the local interstellar spectra of p and He.
- 3He and 4He isotopic composition.

See Claudio Corti presentation.

AMS Daily Proton & Helium Fluxes

The daily flux will give more details on the time evolution of the proton and Helium fluxes (ongoing analysis)

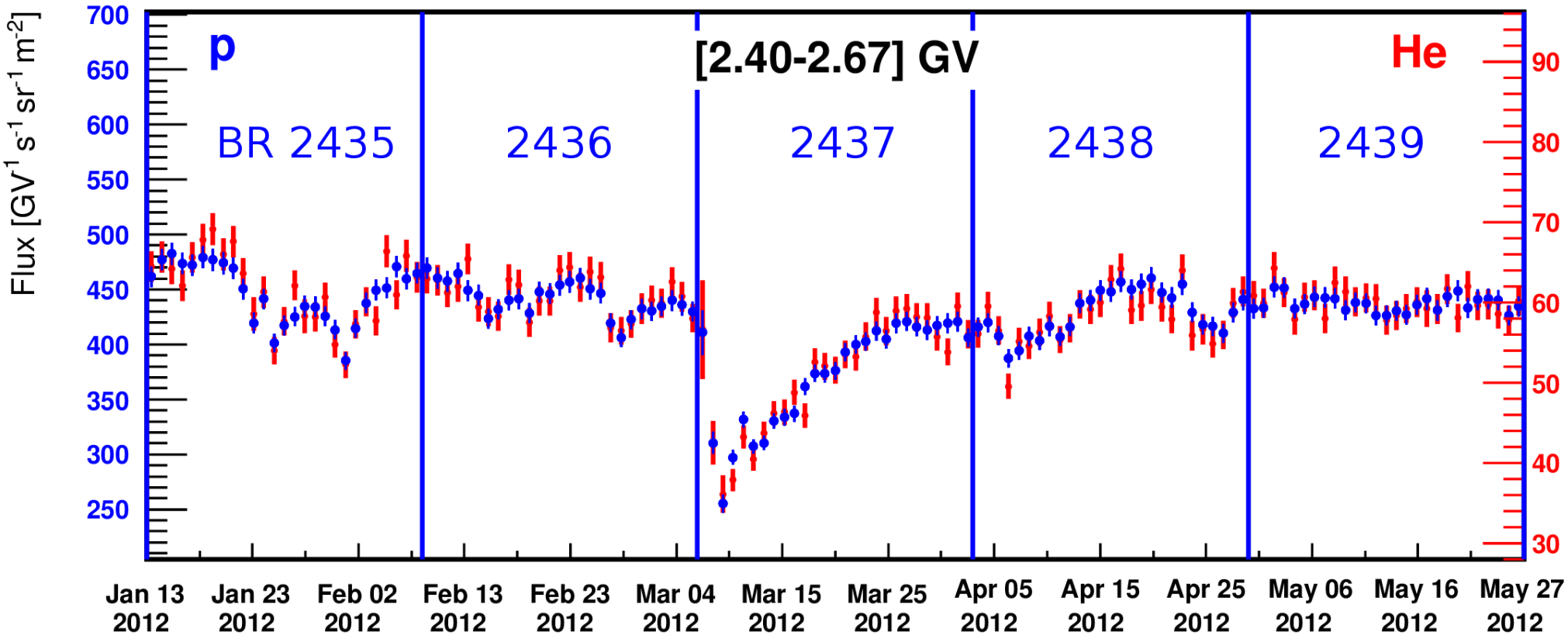

Forbush decreases (FD), Corotating Interaction Regions (CIR), Global Merged Interaction Region (GMIR), and Solar Energetic Particles (SEP) studies.

See Alexis Popkow, Christopher Light, Metteo Palermo presentations.

AMS Leptons: Electron & Positron

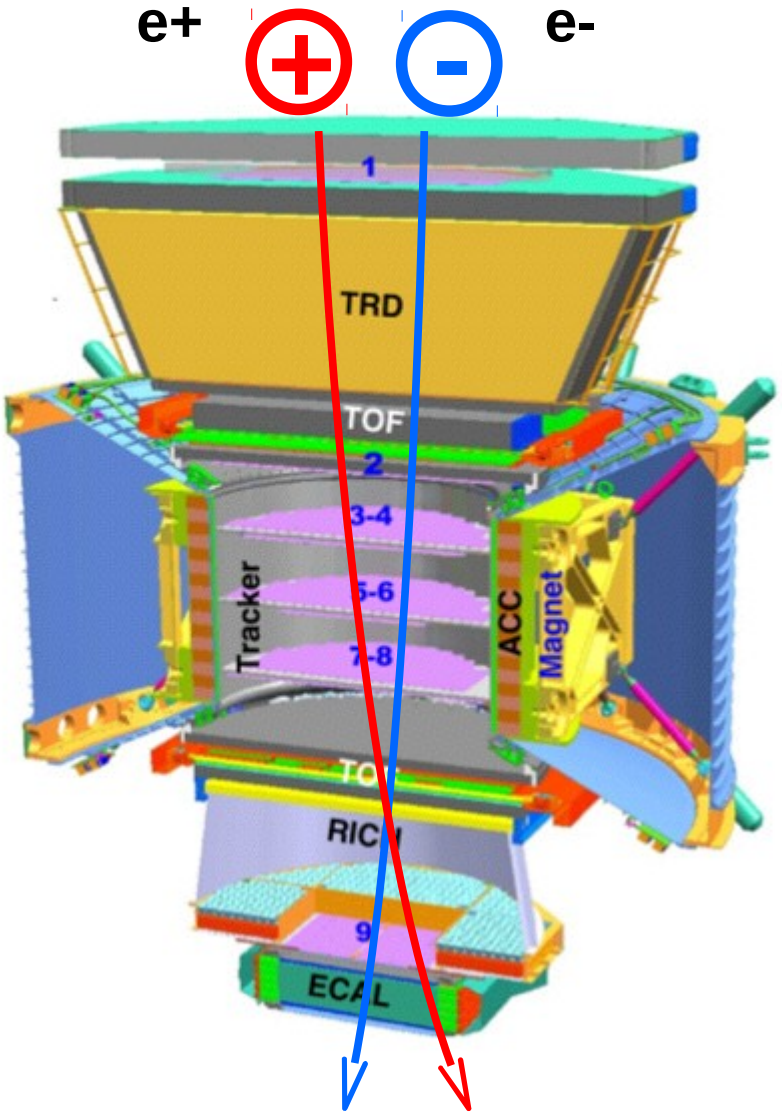

Transition Radiation Detector
- e+ e- identification

Time-of-Flight counter
- Trigger
- Velocity
- Particle flight direction
- Charge

Silicon Tracker + Magnet
- Rigidity
- Charge & sign

Ring Imaging Cherenkov detector
- Velocity
- Charge

Electromagnetic Calorimeter
- e+ e- identification
- e+ e- Energy

AMS Electron and Positron Monthly Fluxes

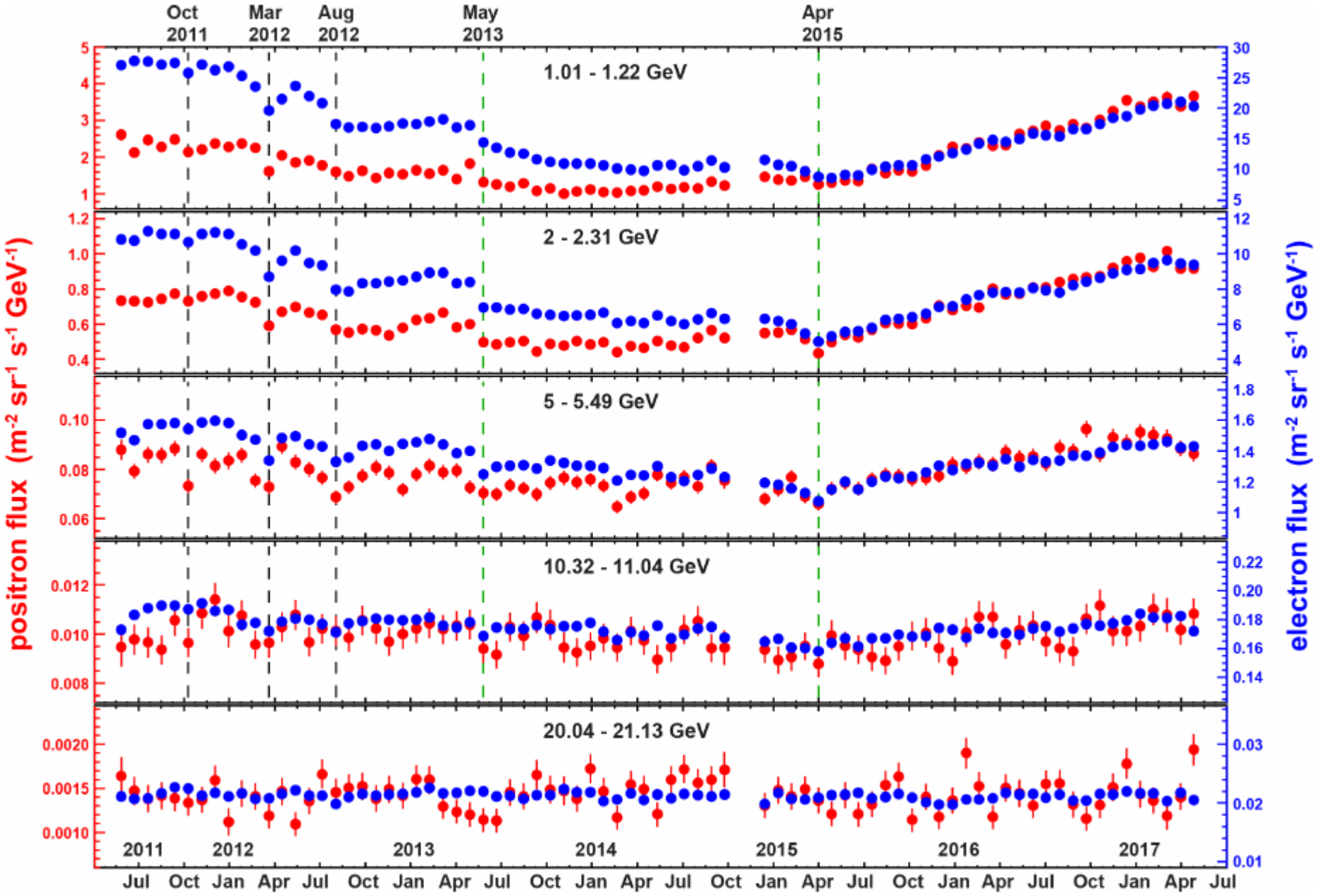

AMS Positron/Electron Flux Ratio

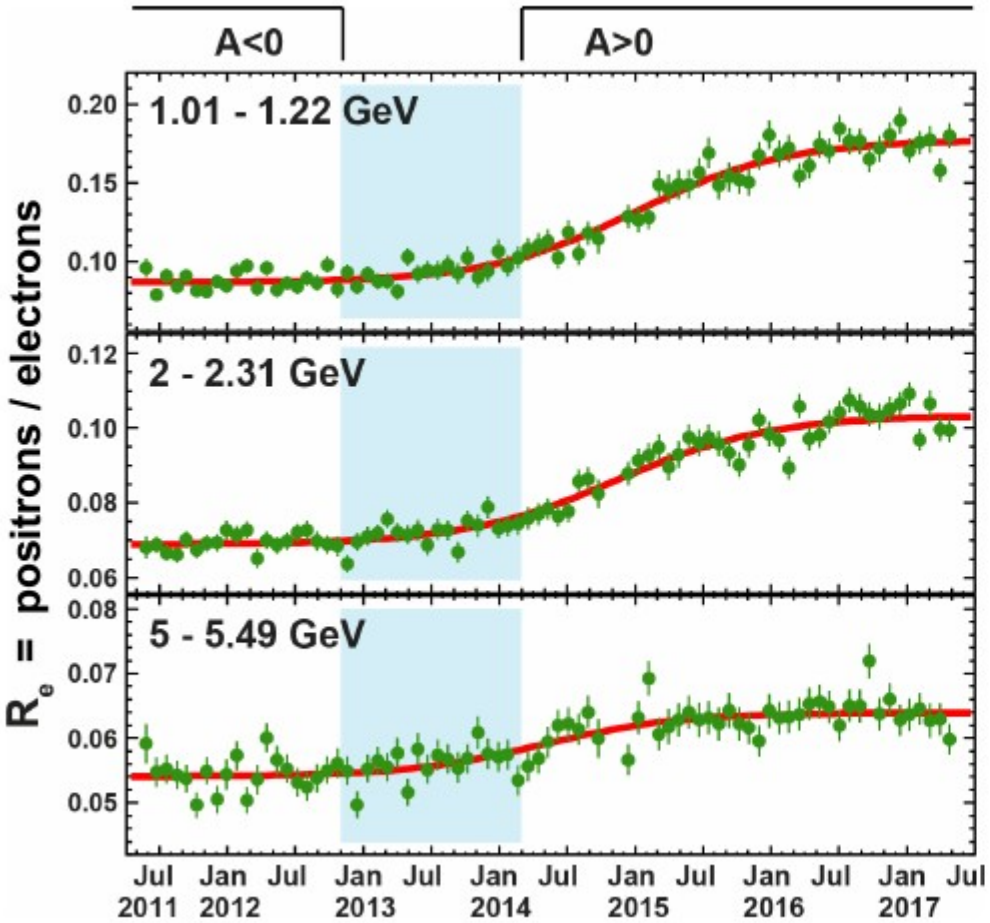

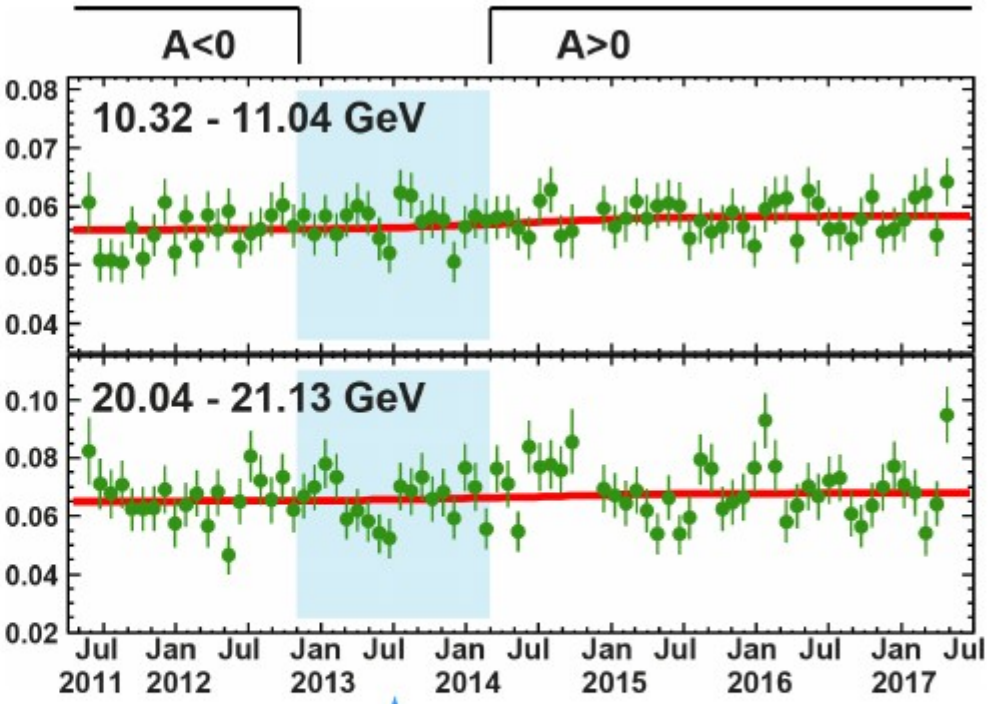

Polarity reversal of solar magnetic field in 2013.

AMS Positron/Electron Transition Parametrization

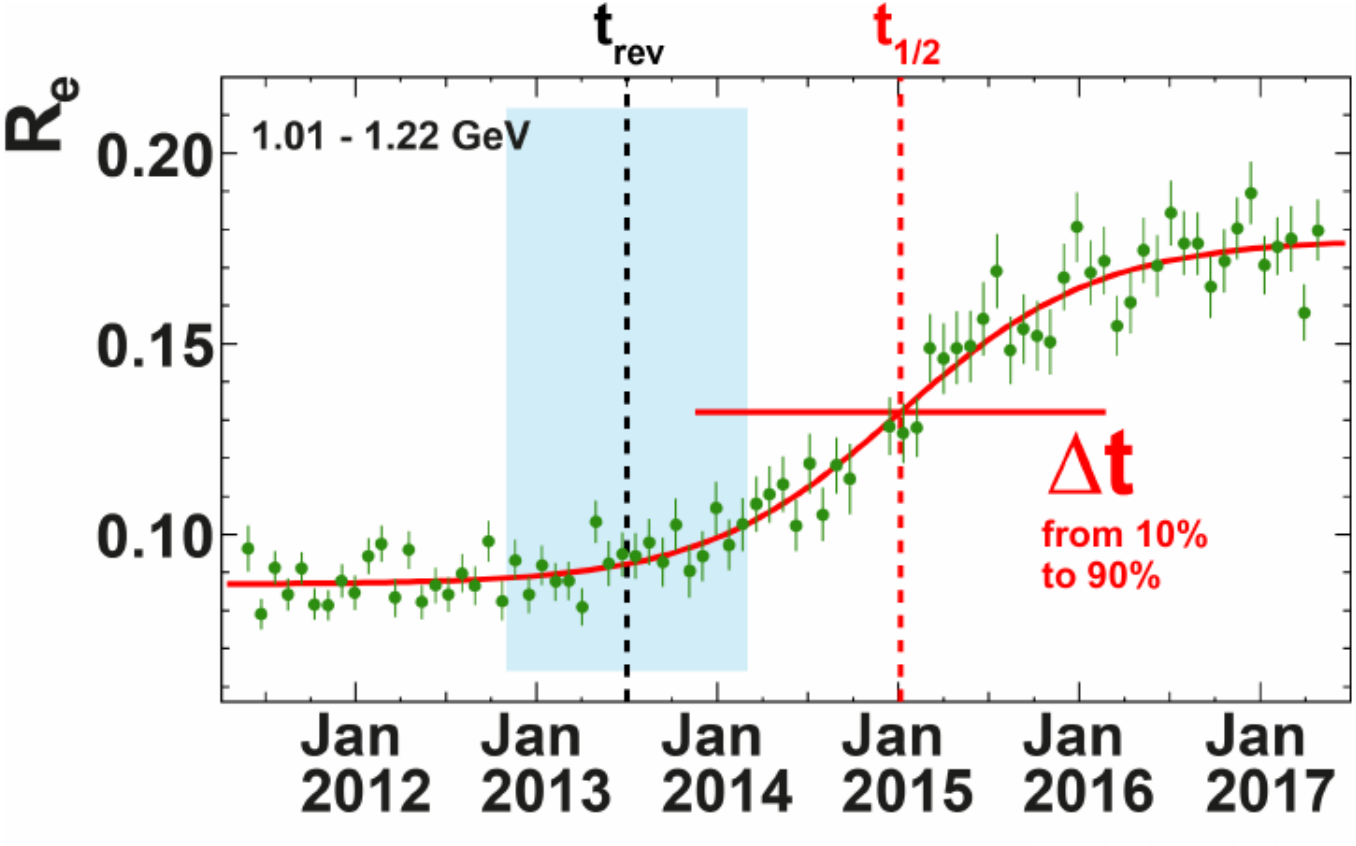

relative amplitude of transition

$$R_e(t,E) = R_0(E)\left[1 + \frac{C(E)}{\exp\left(-\frac{t-t_{1/2}(E)}{\Delta t(E)/\Delta_{80}}\right)+1}\right]$$

duration of transition

midpoint of transition

AMS Positron/Electron Transition Parametrization

$$R_e(t,E) = R_0(E)\left[1 + \frac{C(E)}{\exp\left(-\frac{t-t_{1/2}(E)}{\Delta t(E)/\Delta_{80}}\right)+1}\right]$$

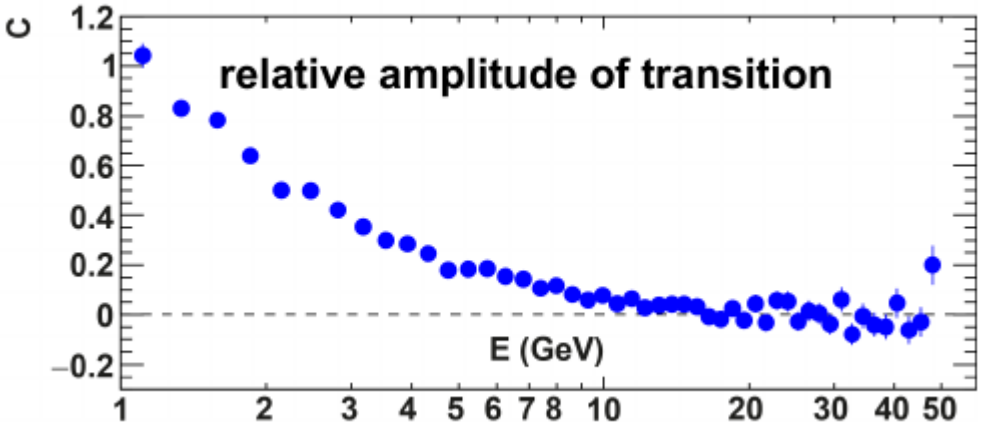

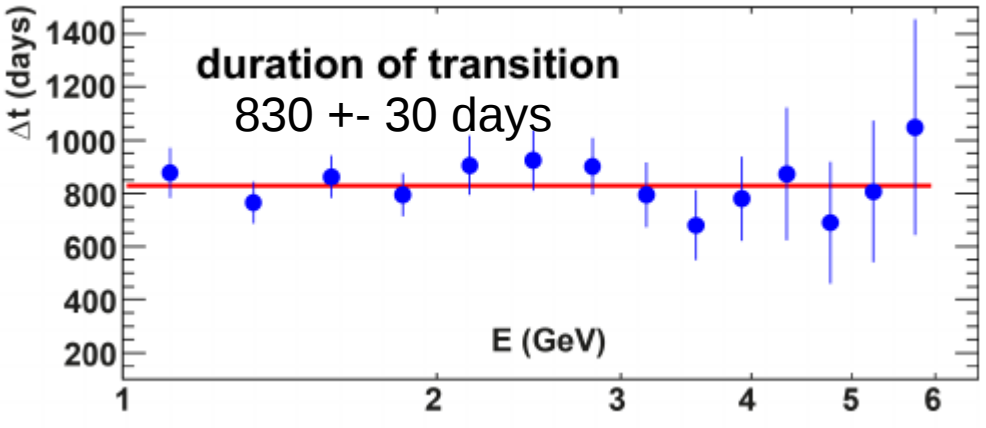

Midpoint of transition changes by (260 ± 30) days from 1 to 6 GeV.

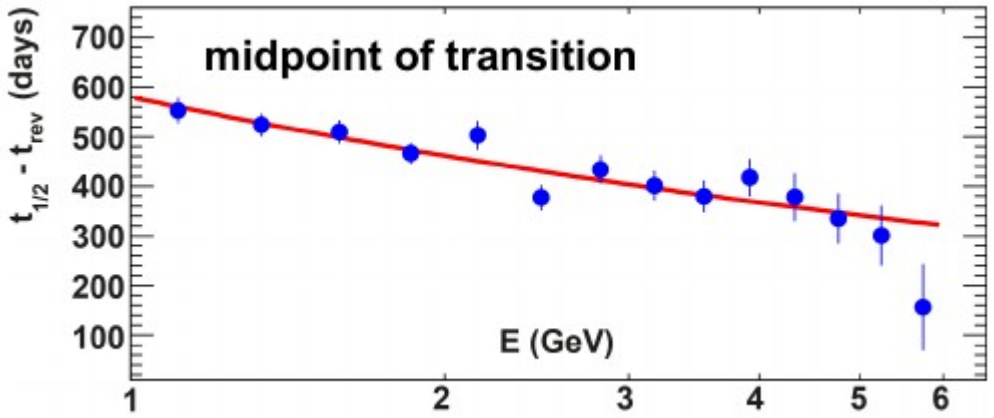

Drift Effect on Opposite Charged Particles

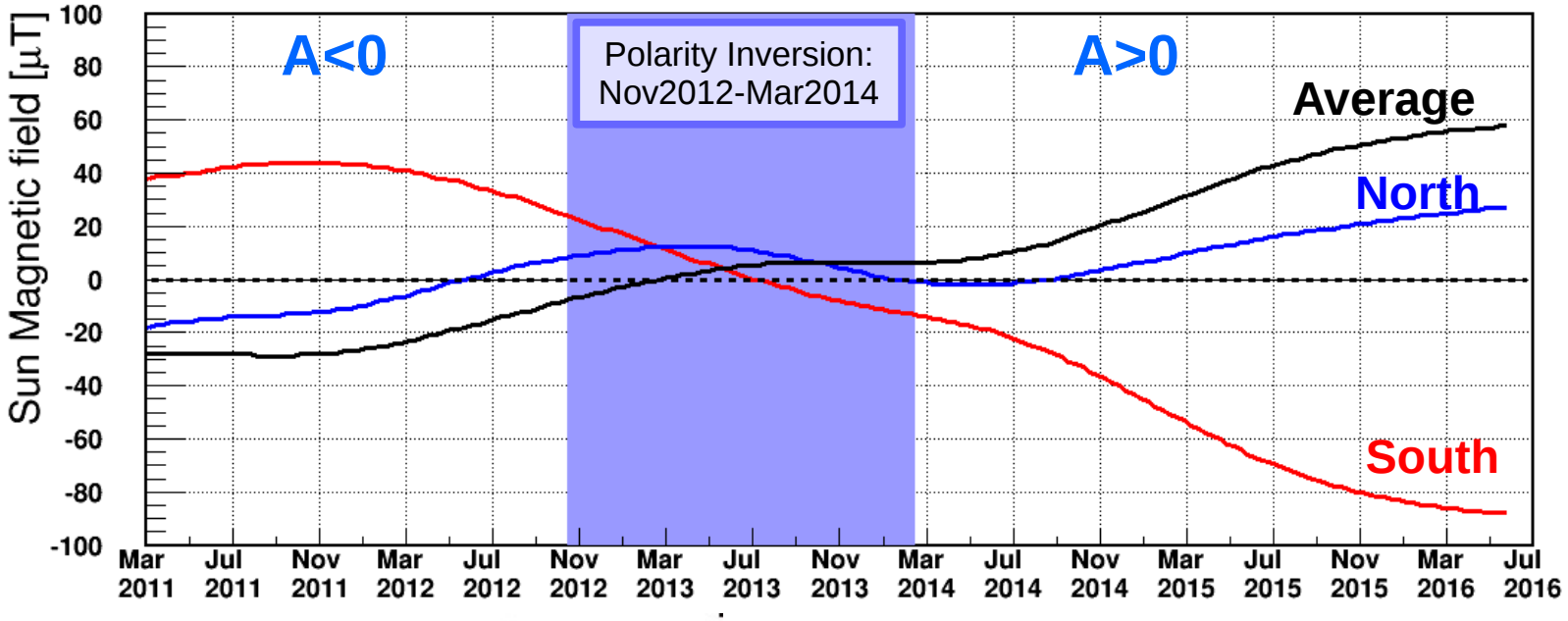

Drift direction of positrons in A>0 epochs or **electrons A<0**

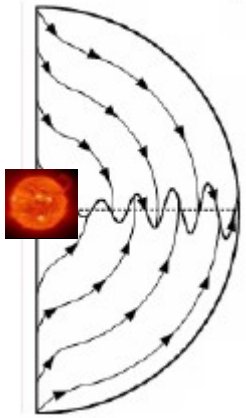

Drift direction of positrons in A<0 epochs or **electrons A>0**

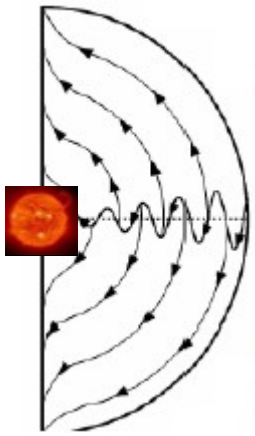

A<0 negative particles are less modulated than positive particles
A>0 negative particles are more modulated than positive particles

Sun's Magnetic filed data from Wilcox Solar Observatory http://wso.stanford.edu/
Polarity inversion period from: X. Sun et al., Astroph. J., 798, 114 (2015)

p&He and e+ e-
Submitted for Publication on PRL

Observation of Fine Time Structures in the Cosmic Proton and Helium Fluxes with the Alpha Magnetic Spectrometer on the International Space Station

M. Aguilar,[27] L. Ali Cavasonza,[1] B. Alpat,[32] G. Ambrosi,[32] L. Arruda,[25] N. Attig,[22] S. Aupetit,[18] P. Azzarello,[17] A. Bachlechner,[1] F. Barao,[25] A. Barrau,[18] L. Barrin,[16] A. Bartoloni,[37] L. Basara,[35] S. Başeğmez-du Pree,[6] M. Battarbee,[45] R. Battiston,[35,36,a] U. Becker,[10] M. Behlmann,[10] B. Beischer,[1] J. Berdugo,[27] B. Bertucci,[32,33] K.F. Bindel,[23] V. Bindi,[20] W. de Boer,[23] K. Bollweg,[21] V. Bonnivard,[18] B. Borgia,[37,38] M.J. Boschini,[29] M. Bourquin,[17] E.F. Bueno,[39] J. Burger,[10] F. Cadoux,[17] X.D. Cai,[10] M. Capell,[10] S. Caroff,[3] J. Casaus,[27] G. Castellini,[15] F. Cervelli,[34] M.J. Chae,[40] Y.H. Chang,[11] A.I. Chen,[10] G.M. Chen,[6] H.S. Chen,[6,7] Y. Chen,[17] L. Cheng,[41] H.Y. Chou,[11] E. Choumilov,[10] V. Choutko,[10] C.H. Chung,[1] C. Clark,[21] R. Clavero,[24] G. Coignet,[3] C. Consolandi,[20] A. Contin,[8,9] C. Corti,[20] W. Creus,[44] M. Crispoltoni,[32,33] Z. Cui,[41] K. Dadzie,[10] Y.M. Dai,[5] A. Datta,[20] C. Delgado,[27] S. Della Torre,[29] M.B. Demirköz,[2] L. Derome,[18] S. Di Falco,[34] F. Dimiccoli,[35,36] C. Díaz,[27] P. von Doetinchem,[20] F. Dong,[31] F. Donnini,[32,33] M. Duranti,[32] D. D'Urso,[32,b] A. Egorov,[10] A. Eline,[10] T. Eronen,[45] J. Feng,[10] E. Fiandrini,[32,33] P. Fisher,[10] V. Formato,[32] Y. Galaktionov,[10] G. Gallucci,[34] R.J. García-López,[24] C. Gargiulo,[16] H. Gast,[1] I. Gebauer,[23] M. Gervasi,[29,30] A. Ghelfi,[18] F. Giovacchini,[27] D. M. Gómez-Coral,[28] J. Gong,[31] C. Goy,[3] V. Grabski,[28] D. Grandi,[29] M. Graziani,[23] K.H. Guo,[19] S. Haino,[44] K.C. Han,[26] Z.H. He,[19] M. Heil,[10] J. Hoffman,[20] T.H. Hsieh,[10] H. Huang,[44,c] Z.C. Huang,[19] C. Huh,[14] M. Incagli,[34] M. Ionica,[32] W.Y. Jang,[14] Yi Jia,[10] H. Jinchi,[26] S.C. Kang,[14] K. Kanishev,[35,16] B. Khiali,[11] G.N. Kim,[14] K.S. Kim,[14] Th. Kirn,[1] C. Konak,[2] O. Kounina,[10] A. Kounine,[10] V. Koutsenko,[10] A. Kulemzin,[10] G. La Vacca,[29,30] E. Laudi,[16] G. Laurenti,[8] I. Lazzizzera,[35,36] A. Lebedev,[10] H.T. Lee,[43] S.C. Lee,[44] C. Leluc,[17] H.S. Li,[42] J.Q. Li,[31] Q. Li,[31] T.X. Li,[19] Z.H. Li,[6] Z.Y. Li,[44,d] C. Light,[20] S. Lim,[14] C.H. Lin,[44] P. Lipari,[37] T. Lippert,[22] D. Liu,[11] Hu Liu,[10,e] V.D. Lordello,[39] S.Q. Lu,[44,d] Y.S. Lu,[6] K. Luebelsmeyer,[1] F. Luo,[41] J.Z. Luo,[31] X. Luo,[20] S.S. Lyu,[19] F. Machate,[1] C. Mañá,[27] J. Marín,[27] T. Martin,[21] G. Martínez,[27] N. Masi,[8] D. Maurin,[18] A. Menchaca-Rocha,[28] Q. Meng,[31] V.M. Mikuni,[39] D.C. Mo,[19] P. Mott,[21] T. Nelson,[20] J.Q. Ni,[19] N. Nikonov,[1] F. Nozzoli,[32,f] A. Oliva,[27] M. Orcinha,[25] M. Palermo,[20] F. Palmonari,[8,9] C. Palomares,[27] M. Paniccia,[17] M. Pauluzzi,[32,33] S. Pensotti,[29,30] C. Perrina,[17] H.D. Phan,[10] N. Picot-Clemente,[13] F. Pilo,[34] C. Pizzolotto,[32,g] V. Plyaskin,[10] M. Pohl,[17] V. Poireau,[3] A. Poplow,[20] L. Quadrani,[8,9] X.M. Qi,[19] X. Qin,[10] Z.Y. Qu,[44,h]

Observation of Complex Time Structures in the Cosmic-Ray Electron and Positron Fluxes with the Alpha Magnetic Spectrometer on the International Space Station

M. Aguilar,[27] L. Ali Cavasonza,[1] G. Ambrosi,[32] L. Arruda,[25] N. Attig,[22] S. Aupetit,[18] P. Azzarello,[17] A. Bachlechner,[1] F. Barao,[25] A. Barrau,[18] L. Barrin,[16] A. Bartoloni,[37] L. Basara,[35] S. Başeğmez-du Pree,[6] M. Battarbee,[45] R. Battiston,[35,36,a] U. Becker,[10] M. Behlmann,[10] B. Beischer,[1] J. Berdugo,[27] B. Bertucci,[32,33] K.F. Bindel,[23] V. Bindi,[20] W. de Boer,[23] K. Bollweg,[21] V. Bonnivard,[18] B. Borgia,[37,38] M.J. Boschini,[29] M. Bourquin,[17] E.F. Bueno,[39] J. Burger,[10] F. Cadoux,[17] X.D. Cai,[10] M. Capell,[10] S. Caroff,[3] J. Casaus,[27] G. Castellini,[15] F. Cervelli,[34] M.J. Chae,[40] Y.H. Chang,[11] A.I. Chen,[10] G.M. Chen,[6] H.S. Chen,[6,7] Y. Chen,[17] L. Cheng,[41] H.Y. Chou,[11] E. Choumilov,[10] V. Choutko,[10] C.H. Chung,[1] C. Clark,[21] R. Clavero,[24] G. Coignet,[3] C. Consolandi,[20] A. Contin,[8,9] C. Corti,[20] W. Creus,[44] M. Crispoltoni,[32,33] Z. Cui,[41] K. Dadzie,[10] Y.M. Dai,[5] A. Datta,[20] C. Delgado,[27] S. Della Torre,[29] M.B. Demirköz,[2] L. Derome,[18] S. Di Falco,[34] F. Dimiccoli,[35,36] C. Díaz,[27] P. von Doetinchem,[20] F. Dong,[31] F. Donnini,[32,33] M. Duranti,[32] D. D'Urso,[32,b] A. Egorov,[10] A. Eline,[10] T. Eronen,[45] J. Feng,[10] E. Fiandrini,[32,33] P. Fisher,[10] V. Formato,[32] Y. Galaktionov,[10] G. Gallucci,[34] R.J. García-López,[24] C. Gargiulo,[16] H. Gast,[1] I. Gebauer,[23] M. Gervasi,[29,30] A. Ghelfi,[18] F. Giovacchini,[27] D. M. Gómez-Coral,[28] J. Gong,[31] C. Goy,[3] V. Grabski,[28] D. Grandi,[29] M. Graziani,[23] K.H. Guo,[19] S. Haino,[44] K.C. Han,[26] Z.H. He,[19] M. Heil,[10] T.H. Hsieh,[10] H. Huang,[44,c] Z.C. Huang,[19] C. Huh,[14] M. Incagli,[34] M. Ionica,[32] W.Y. Jang,[14] Yi Jia,[10] H. Jinchi,[26] S.C. Kang,[14] K. Kanishev,[35,16] B. Khiali,[11] G.N. Kim,[14] K.S. Kim,[14] Th. Kirn,[1] C. Konak,[2] O. Kounina,[10] A. Kounine,[10] V. Koutsenko,[10] A. Kulemzin,[10] G. La Vacca,[29,30] E. Laudi,[16] G. Laurenti,[8] I. Lazzizzera,[35,36] A. Lebedev,[10] H.T. Lee,[43] S.C. Lee,[44] C. Leluc,[17] H.S. Li,[42] J.Q. Li,[31] Q. Li,[31] T.X. Li,[19] Z.H. Li,[6] Z.Y. Li,[44,d] S. Lim,[14] C.H. Lin,[44] P. Lipari,[37] T. Lippert,[22] D. Liu,[11] Hu Liu,[10] V.D. Lordello,[39] S.Q. Lu,[44,d] Y.S. Lu,[6] K. Luebelsmeyer,[1] F. Luo,[41] J.Z. Luo,[31] S.S. Lyu,[19] F. Machate,[1] C. Mañá,[27] J. Marín,[27] T. Martin,[21] G. Martínez,[27] N. Masi,[8] D. Maurin,[18] A. Menchaca-Rocha,[28] Q. Meng,[31] V.M. Mikuni,[39] D.C. Mo,[19] P. Mott,[21] T. Nelson,[20] J.Q. Ni,[19] N. Nikonov,[1] F. Nozzoli,[32,35,e] A. Oliva,[27] M. Orcinha,[25] M. Palermo,[20] F. Palmonari,[8,9] C. Palomares,[27] M. Paniccia,[17] M. Pauluzzi,[32,33] S. Pensotti,[29,30] C. Perrina,[17] H.D. Phan,[10] N. Picot-Clemente,[13] F. Pilo,[34] C. Pizzolotto,[32,f] V. Plyaskin,[10] M. Pohl,[17] V. Poireau,[3] L. Quadrani,[8,9] X.M. Qi,[19] X. Qin,[10] Z.Y. Qu,[44,g] T. Räihä,[1] P.G. Rancoita,[29] D. Rapin,[17] J.S. Ricol,[18] S. Rosier-Lees,[3] A. Rozhkov,[10]

AMS particle and antiparticle: Proton & Anti-proton

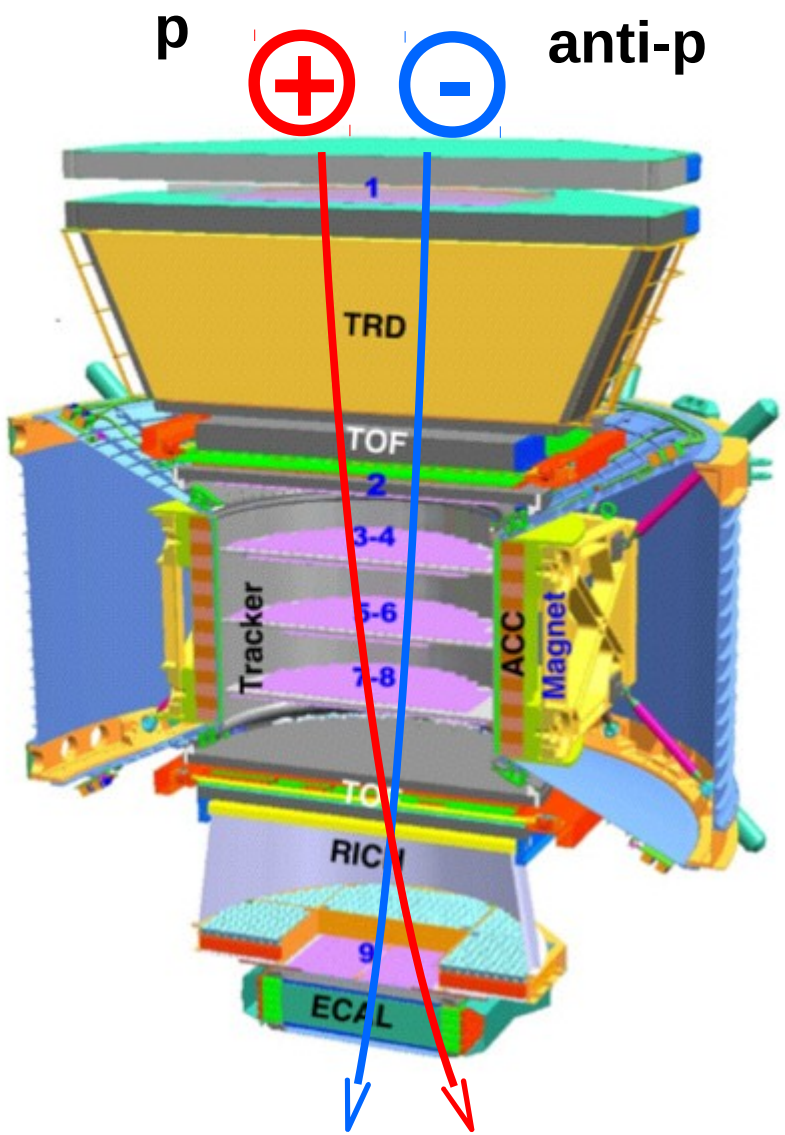

Transition Radiation Detector
- to separate anti-p and p from e+ and e-

Time-of-Flight counter
- Trigger
- Velocity
- Particle flight direction
- Charge

Silicon Tracker + Magnet
- Rigidity
- Charge & sign

Ring Imaging Cherenkov detector
- Velocity
- Charge
- to separate anti-p and p from other |Z|=1

Electromagnetic Calorimeter
- to separate anti-p and p from e+ and e-

AMS Proton/Anti-proton Flux Ratio

From May 2011 to Nov 2016, each point is 81 days of integration

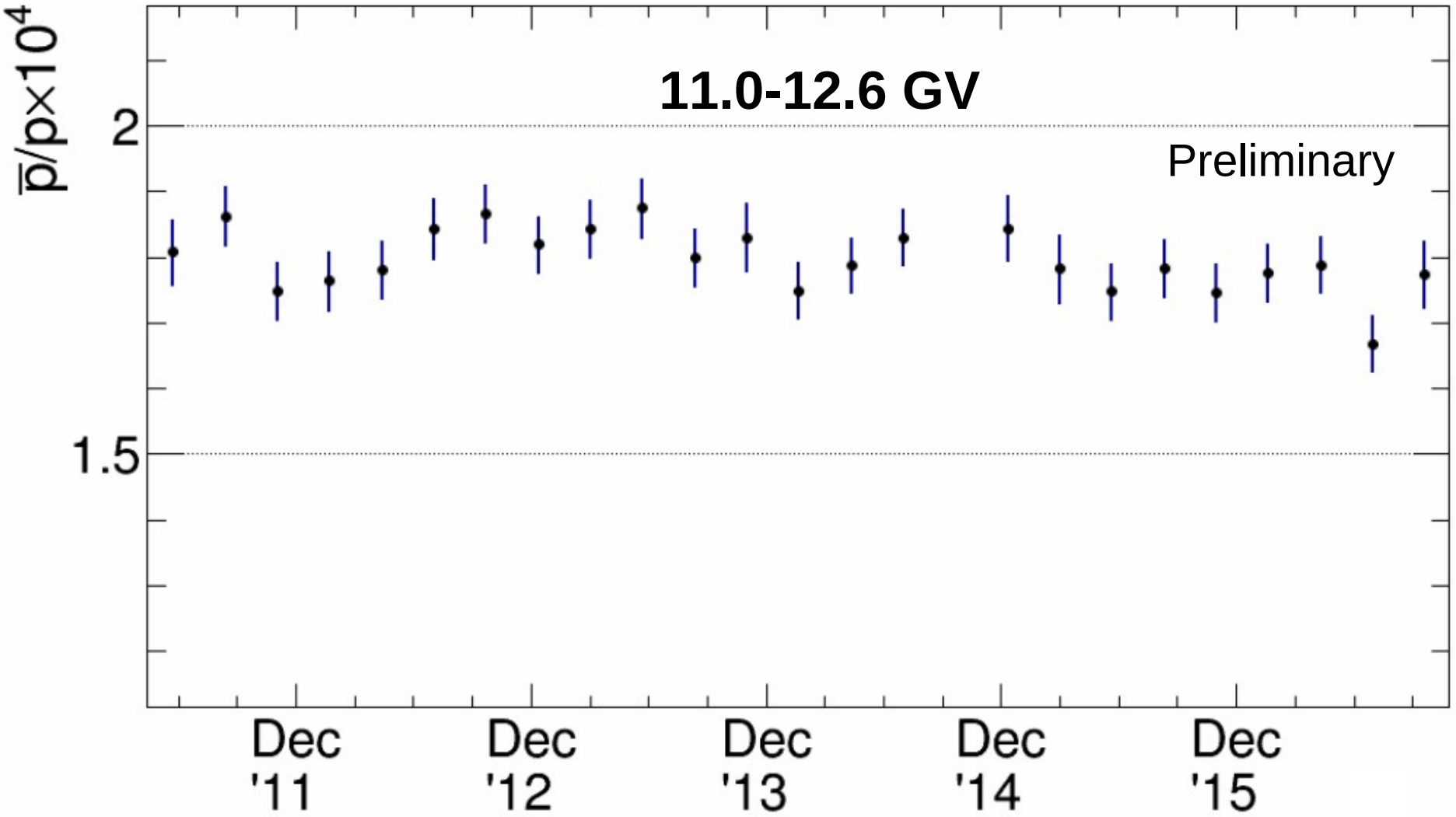

AMS Proton/Anti-proton Flux Ratio

From May 2011 to Nov 2016, each point is 81 days of integration

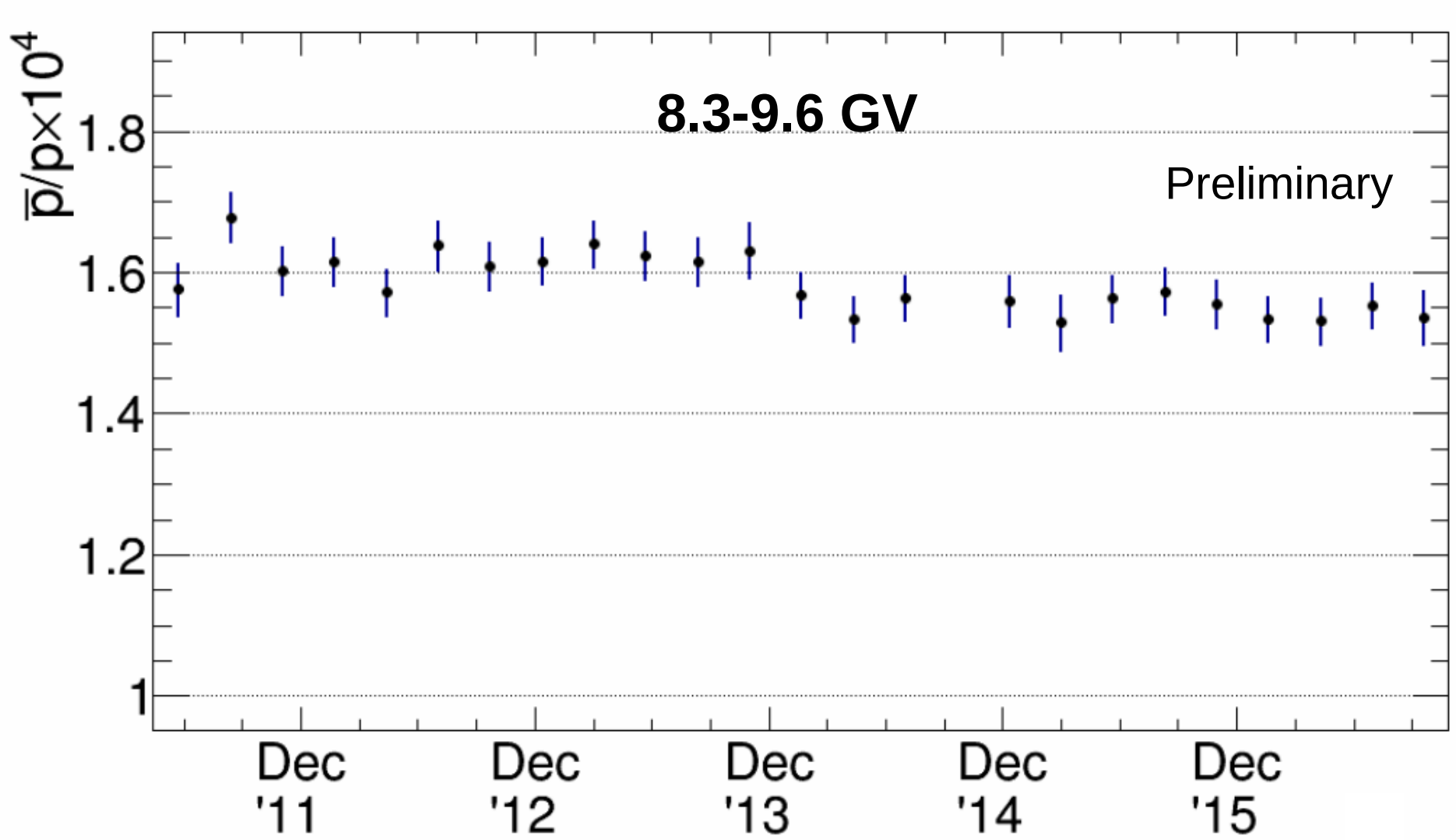

AMS Proton/Anti-proton Flux Ratio

From May 2011 to Nov 2016, each point is 81 days of integration

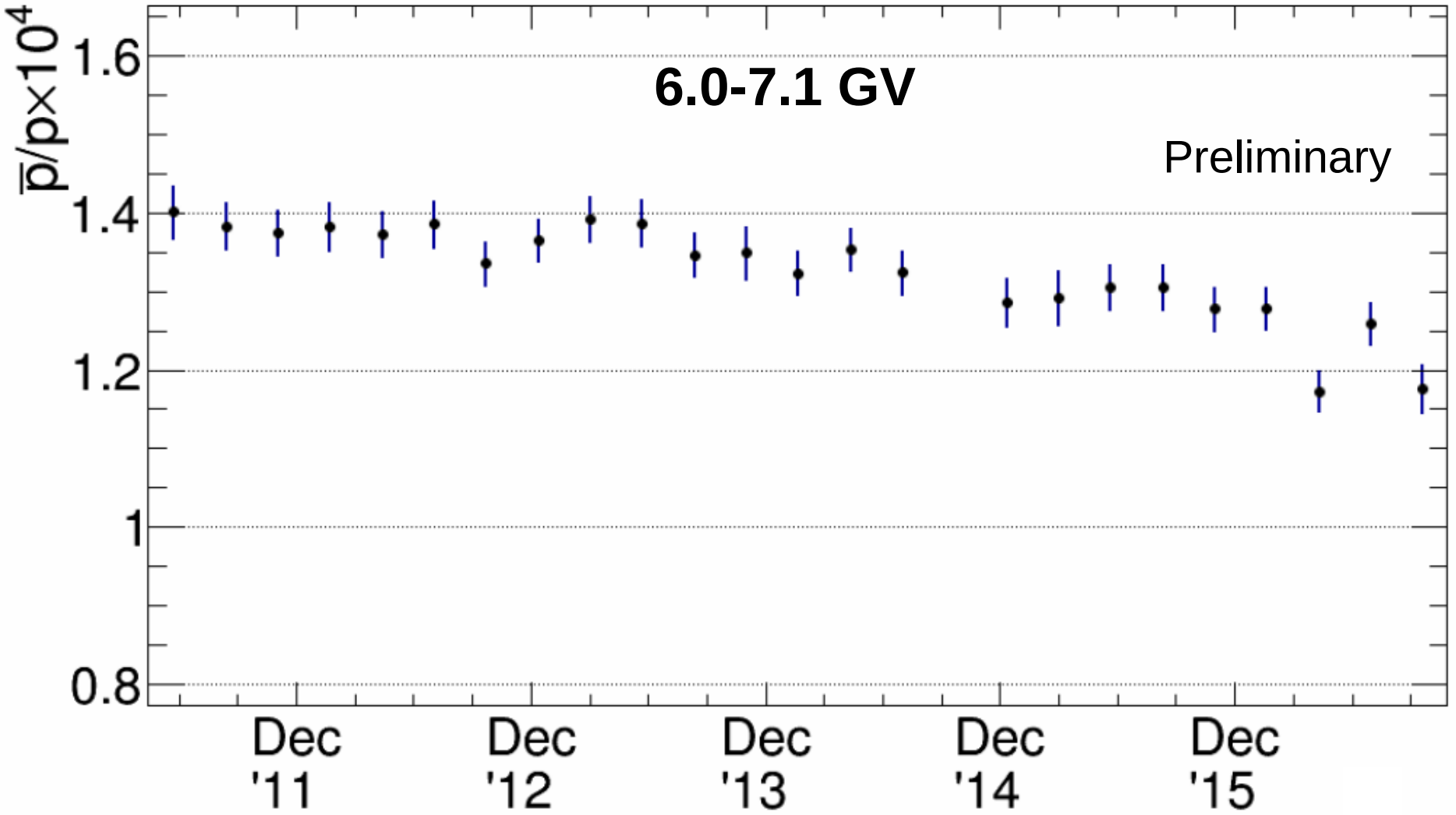

AMS Proton/Anti-proton Flux Ratio

From May 2011 to Nov 2016, each point is 81 days of integration

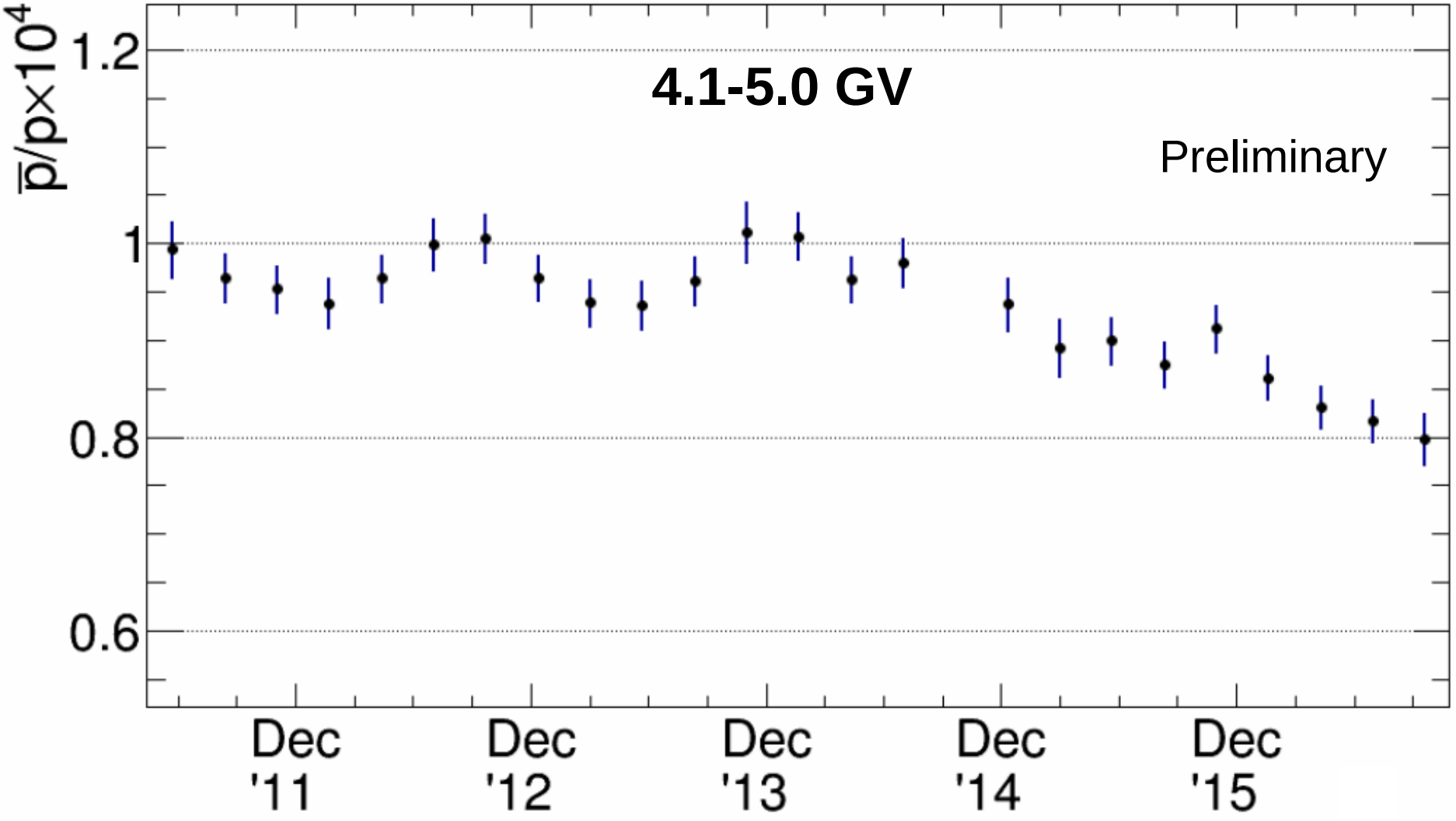

AMS Proton/Anti-proton Flux Ratio

From May 2011 to Nov 2016, each point is 81 days of integration

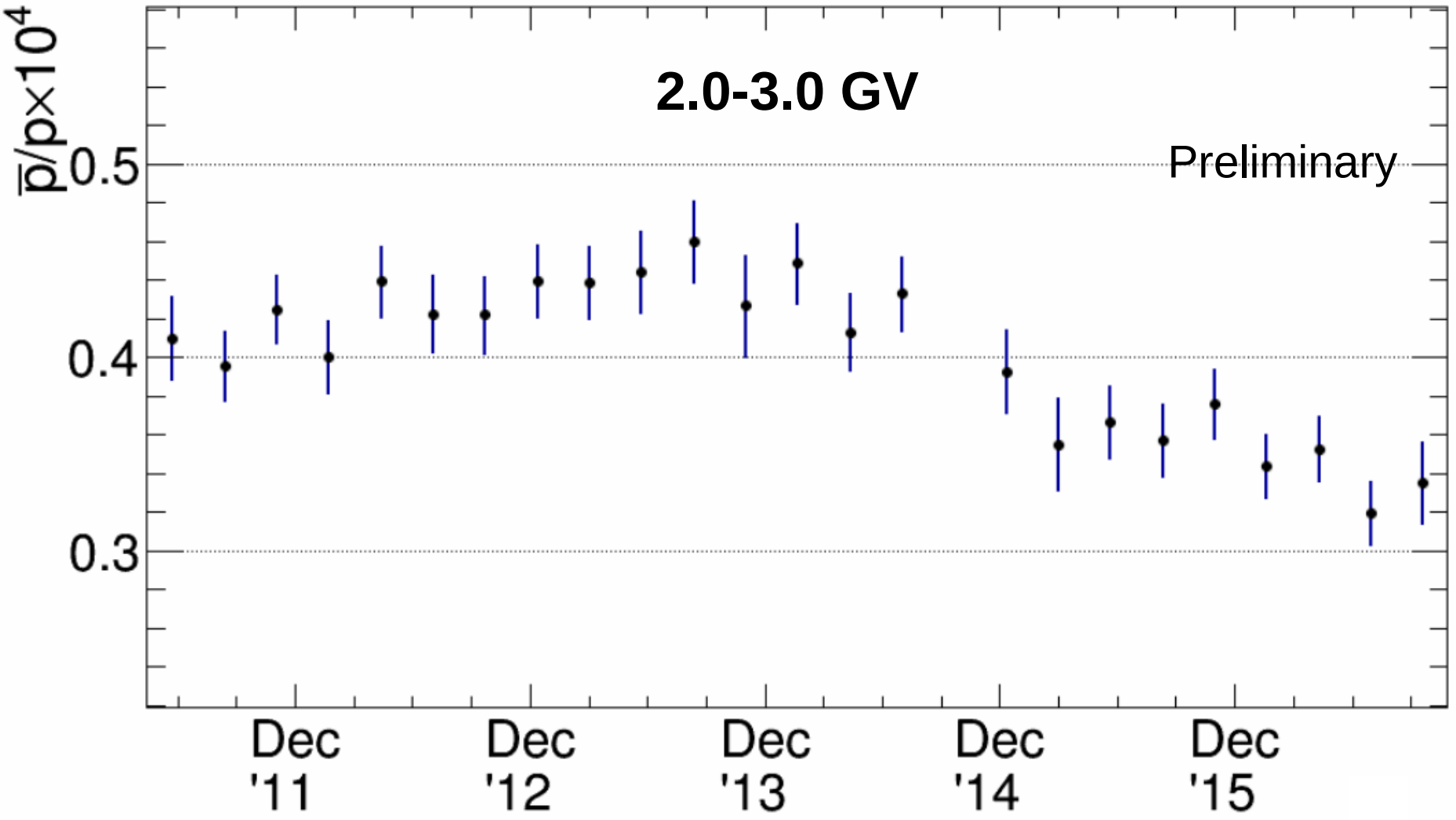

AMS Proton/Anti-proton Flux Ratio

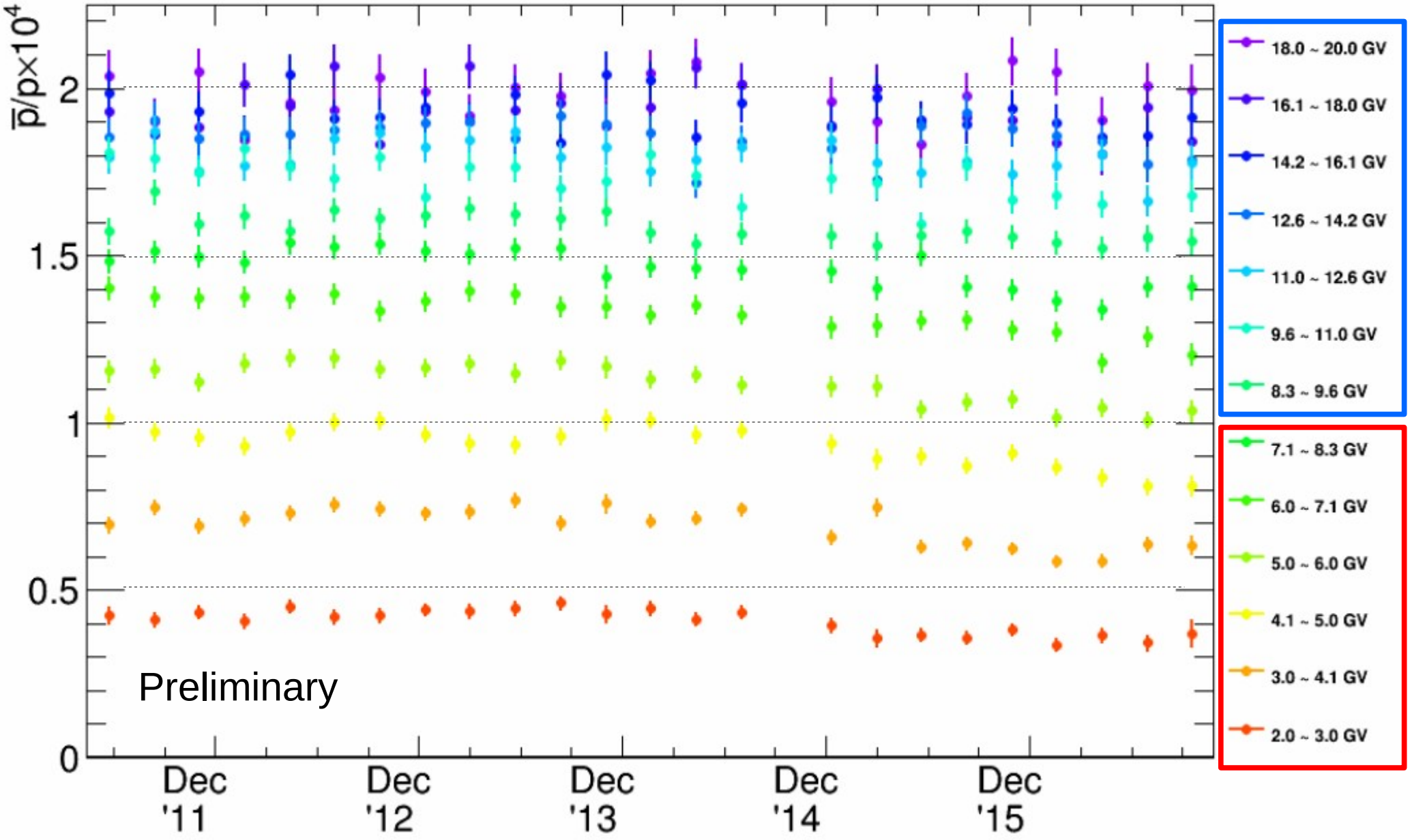

Summary & Conclusions

- AMS p, He, e+,e-, anti-p monthly fluxes were measured during the ascending phase of solar cycle 24 through its maximum and toward its minimum.
- Fluxes at low rigidity show sub-structures related to the short-term solar activity.
- Above 3 GV the p/He flux ratio is time independent while below 3 GV the p/He flux ratio has a long-term decrease
- AMS e+/e- and anti-p/p ratio clearly shows the charge-sign dependence of solar modulation.
- AMS is measuring all nuclei, particle and anti-particle fluxes in the present and next solar cycle.

Backup

Time Evolution of Spectral Indices at 10GV

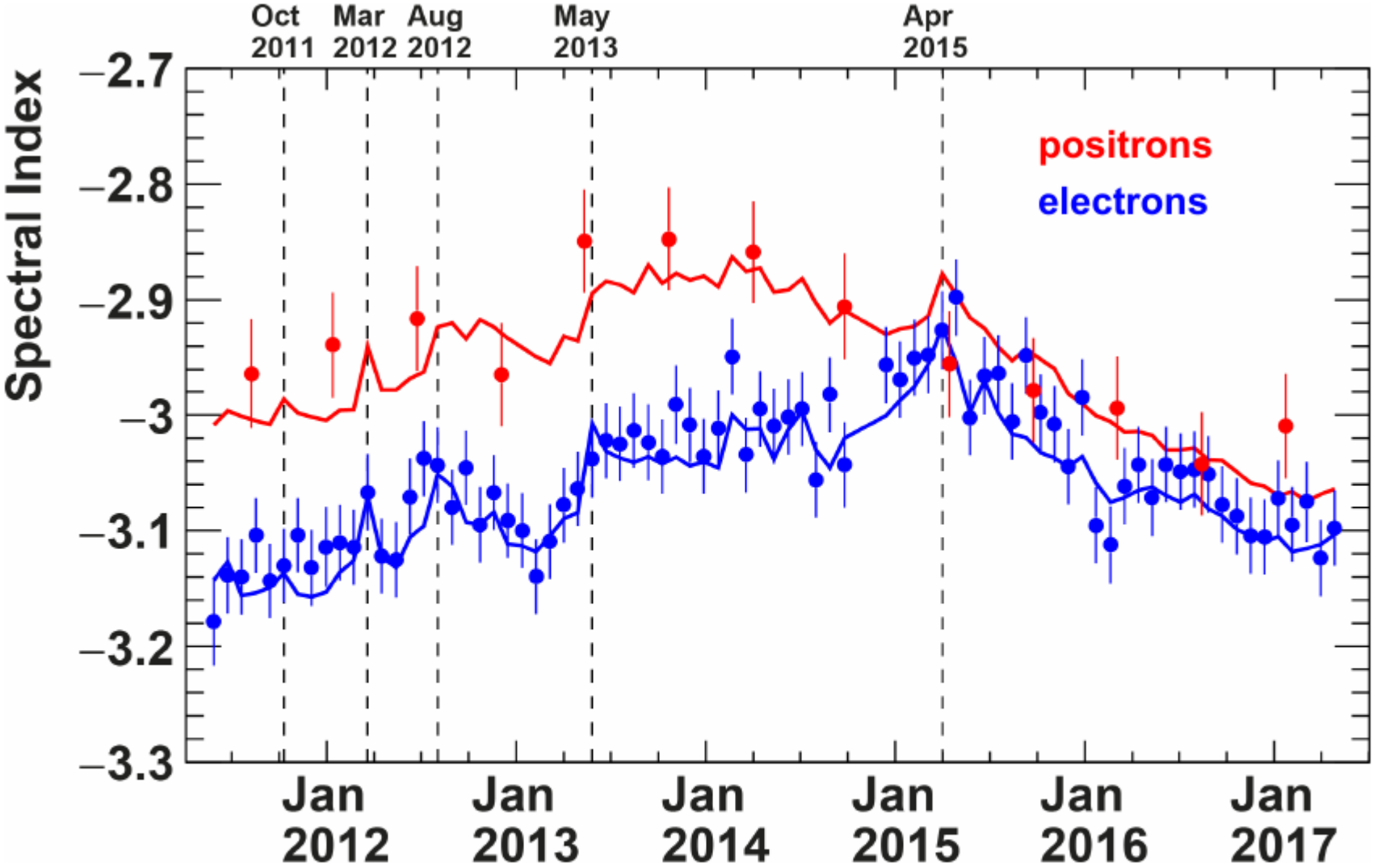

Spectral indices for both positrons and electrons harden until April 2015, then soften with identical slope.